INVESTIGATING THE REGULATORY ROLE OF LYSOSOMAL PROTEIN CATHEPSIN A IN VASOACTIVE PEPTIDE BIOLOGY

A Thesis Submitted to
the Graduate School of Engineering and Sciences of
İzmir Institute of Technology
in Partial Fulfillment of the Requirements for the Degree of

MASTER OF SCIENCE

in Molecular Biology and Genetics

by

Osman Yipkin ÇALHAN

July 2016
İzmir

We approve the thesis of **Osman Yipkin ÇALHAN**

Examining Committee Members

_____
Prof. Dr. Volkan SEYRANTEPE
Department of Molecular Biology and Genetics, İzmir Institute of Technology

_____
Assoc. Prof. Dr. Bünyamin AKGÜL
Department of Molecular Biology and Genetics, İzmir Institute of Technology

_____
Assoc. Prof. Dr. Michelle M. ADAMS
Department of Psychology, Bilkent University

26 July 2016

_____
Prof. Dr. Volkan SEYRANTEPE
Supervisor, Department of Molecular Biology and Genetics,
İzmir Institute of Technology

_____   _____
Prof. Dr. Volkan SEYRANTEPE   **Prof. Dr. Bilge KARAÇALI**
Head of Department of Molecular   Dean of Graduate School of
Biology and Genetics   Engineering and Sciences

ACKNOWLEDGEMENTS

ABSTRACT

INVESTIGATING THE REGULATORY ROLE OF LYSOSOMAL PROTEIN CATHEPSIN A IN VASOACTIVE PEPTIDE BIOLOGY

The lysosomal carboxypeptidase A, Cathepsin A (CathA), is a serine protease with distinct functions. CathA protects sialidase Neu1 and β- galactosidase against proteolytic degradation by forming a multi-enzyme complex and was shown to be activating sialidase Neu1. Mutations in the CathA gene cause the lysosomal storage disease galactosialidosis. Patients with galactosialidosis are characterized with a broad range of clinical phenotypes, involving growth retardation, neurological deterioration and accumulation of vasoactive peptide, endothelin-1 in the brain. CathA is also a multi-catalytic enzyme with deamidase and esterase activity at neutral pH, and carboxypeptidase activity at acidic pH. Previous investigations have presented that CathA has specific enzyme activity against vasoactive and neuropeptides, including endothelin-1, oxytocin and substance P. A generated mouse model with inactive CathA enzyme activity (CathA^{S190A}) showed significantly increased level of precursor endothelin-1 vasoactive peptide with increased arterial blood pressure. The aim of this study was to ascertain the regulatory role of CathA against other vasoactive peptide precursors such as oxytocin, endothelin-1 and substance P *in vivo*. In addition to the regulatory role of the enzyme, CathA's involvement in learning ability, long term memory and motor cortex functioning was elucidated. Our results showed that CathA has a regulatory role on endothelin-1 and oxytocin peptides' degradation, which is the reason of the increased accumulation in the brain hippocampus region for CathA^{S190A}. Memory based Morris' water maze and passive avoidance tests illustrated that CathA^{S190A} animals had lower scores than control littermates, which let us to speculate that CathA may play significant role in memory consolidation and learning ability through its regulatory role on vasoactive peptide biology.

Keywords: Cathepsin A, vasoactive, peptide, memory

ÖZET

LİZOZOMAL KATEPSİN A PROTEİNİNİN VAZOAKTİF PEPTİD BİYOLOJİSİNDEKİ DÜZENLEYİCİ ROLÜNÜN ARAŞTIRILMASI

Lizozomal karboksipeptidaz A, Katepsin A, birbirinden farkli fonksiyonları olan bir serine proteinazıdır. Katepsin A'nın Neu1 ve beta- galaktosidaz sialidazlarını proteolitik yıkıma karşı çoklu enzim kompleksi oluşturarak koruduğu ve de Neu1'nı aktive ettiği gösterilmiştir. Katepsin A genindeki mutasyonlar lizozomal depo hastalığı galaktosialidosise neden olur. Galaktosialidosis hastaları geç gelişim, sinirsel bozulmalar ve beyin içinde vazoaktif peptit, endotelin-1, birikmesinide içeren geniş aralıkta kliniksel fenotipler ile karakterize edilir. Katepsin A'nın aynı zamanda nötral pH'da deamidaz ve esteraz aktivitesi ile birlikte asidik pH' de karboksipeptidaz aktivitesi olan çoklu- katalitik bir enzimdir. Daha önceki araştırmalar Katpsin A'nın endotelin-1, oksitosin ve substance P'yi de içeren vazoaktif ve nöroaktif peptitlere karşı spesifik enzim aktivitesine sahip olduğunu sunmuştur. İnaktif enzim aktivitesi ile yaratılan Katepsin A fare modeli ($CathA^{S190A}$) öncü vazoaktif endotelin-1' ile atardamar kan basıncının önemli seviyelere yükseldiğini kanıtlamıştır. Bu çalışmanın amacı Katepsin A'nın endotelin-1, oksitosin ve substans P'yi içeren diğer öncü vazoaktif peptitlerine karşı düzenleyici rolünün araştırılarak canlı organizmada ortaya çıkarılmasıdır. Enzimin düzenleyici rolüne ek olarak, Katepsin A öğrenme becerisine, uzun dönem hafıza ve motor korteks fonksiyonlarına olan katılımının ortaya çıkarılmasıdır. Sonuçlarımız gösteriyor ki Katepsin A endotelin-1 ve oksitosin peptitlerinin yıkımı üzerine düzenleyici etkisi vardır, bu da $CathA^{S190A}$'nın beyin hipokampus bölgesindeki artan birikimin sebebidir. Hafıza temelli Morris'in su labitenti ve pasif sakınma testlerinde $CathA^{S190A}$'nın kontrol kardeşlerimden daha düşük sonuçlara sahip olduğunu göstermiştir, bu da bizi Katepsin A'nın hafızada saklama ve öğrenme becerisinde vazoaktif peptit biyoloji sayesinde önemli rolu olabileceğini speküle etmemizi sağlıyor.

Anahtar Kelimeler: Katepsin A, vasoaktif, peptid, hafıza

TABLE OF CONTENTS

LIST OF FIGURES

LIST OF TABLES

CHAPTER 1

INTRODUCTION

1.1 The Lysosome

Nearly half a century ago, Christian de Duve introduced lysosomes as "suicide bags". Lysosomes are membrane- enclosed cytoplasmic organelles found in eukaryotic cells. Lysosomal vesicles contain a broad range of hydrolases considered to play essential roles in intracellular protein degradation and the breakdown of all types of biological polymers (de Duve et al. 1959).

Lysosomes are able to store hydrolases, which degrade materials taken up from outside the cell into their building blocks at the acidic pH 3.8-5 by different digestive methods such as endocytosis and autophagy. In endocytosis the material to be internalized is surrounded by plasma membrane, which later buds off inside the cell to allow digestion of the material by enzymes. In autophagy, a cell gradually digests its own components by enclosing it in an organelle derived from the endoplasmic reticulum. Enclosed vesicular structures fuse with lysosomes to digest the contents. In a lysosome, numerous biological macromolecules are degraded by at least 50 different acid proteases, including cathepsins (Turk & Turk 2009).

Mutations in the genes that encode digestive enzymes are the cause of more than 30 different lysosomal storage disorders, due to the accumulation of material supposed to be degraded within the lysosome. Most of these diseases are the result of deficiencies in single lysosomal enzymes. For example, Galactosialidosis (one of the most common of these disorders) results from a mutation in the gene that encodes the lysosomal enzyme Cathepsin A. Cathepsin A is responsible for the degradation of many vasoactive peptides, such as endothelin-1, angiotensin and vasopressin, and neuropeptides including Oxytocin or Substance P. Cathepsin A also plays a protective role for other enzymes by forming multi-enzyme complexes that prevent their degradation, thus mutations in Cathepsin A can also lead to secondary deficiencies of other enzymes,

causing other lysosomal storage disorders (Cooper & Hausman 2000). In addition to these disorders, aberrations in lysosomal proteolytic mechanisms underlie various diseases, including cancer, inflammatory diseases, obesity, cardiovascular diseases and neurodegenerative disorders (Stoka et al. 2016).

1.2 Proteases

Proteases are enzymes that convert long peptides into amino acids by the digestion of peptide bonds. Degradation of proteins in the lysosome requires specific proteases, namely hydrolases, to work in great harmony. Based on their mechanism of catalytic group in the active site, proteases can be divided into six distinct classes: aspartic, glutamic, metalloproteases, cysteine, serine and threonine proteases (Table 1.1) (López-Otín & Bond 2008; Siklos et al. 2015). They can influence cell proliferation, cell differentiation, DNA replication, transcription, post-translational processing, cellular regulation and can alter the structural integrity of proteins, resulting in the altered function of the substrates (Stoka et al. 2016).

Each enzyme uses the product of the previous enzyme on the pathway as a substrate. As enzymatic members of these pathways must be able to react rapidly and appropriately to dynamically changing substrate conditions in the environment, these pathways must be under the control of tight regulations. Degradation of glycosphingolipids, glycosaminoglycans, oligosaccharides and glycoproteins into smaller subunits by lysosomal hydrolases are examples of such mechanisms. Carboxypeptidase Cathepsin A, which is a member of protease family, forms multi enzyme complex in lysosomes with glycosidase neuraminidase-1 and β-galactosidase (Bonten et al. 2014).

Table 1.1 Classification of proteases based on their catalytic groups.
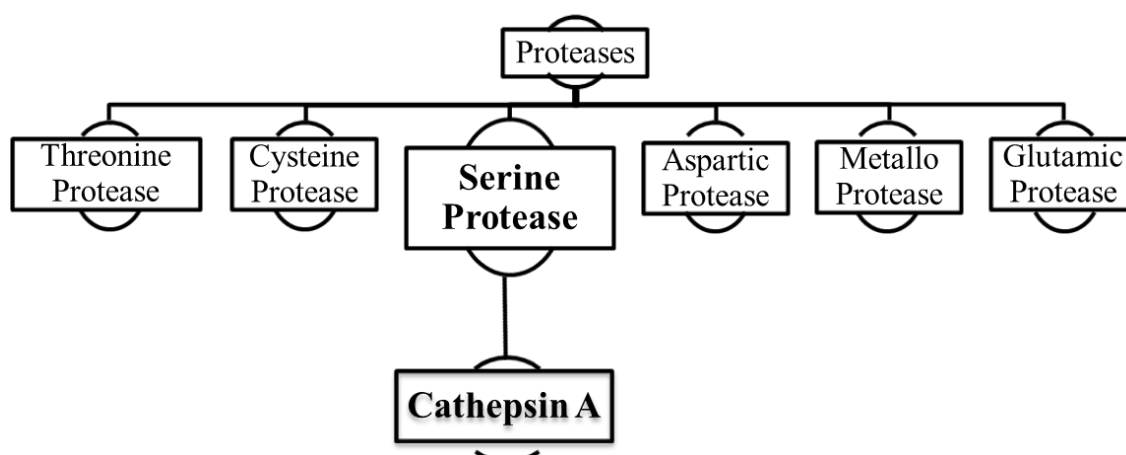
1.3 Cathepsins

In the first half of the 20th century, cathepsins were discovered in the cell lysosome, a group of protease enzymes with several members ubiquitously expressed in the organism. Cathepsins A and G are serine proteases, cathepsins D and E are aspartate proteases; the remainder B, C, F, H, K, L, O, S, V, X and W2 are lysosomal cysteine proteases. Eleven cysteine cathepsins have been discovered in humans – B, C, F, H, K, L, O, S, V, W, and X. The expression and localization profiles of these enzymes vary in different cells and tissues. Although cathepsins belonging to the same group show similarities in structure and biochemical properties, e.g. sharing the same core structure and establishing active forms within the same range of pK_a values (3.5-8.0), their substrate specificities varies (Turk et al. 2001).

1.4 Cathepsin A

Lysosomal Protective Protein/ Cathepsin A (PPCA/CathA) is a ubiquitously expressed component of a lysosomal multi-enzyme complex (LMC) with independent protective and catalytic function (Galjart et al. 1991). The human CathA gene localizes on the long (q) arm of chromosome 20 at position 13.1. (Bonten et al. 2014). CathA precursor is processed by a trypsin-like protease at an acidic pH by the removal of a 20 amino acid linker peptide located between two subunits held by disulfide bonds. Removing of linker peptide divides the 54-kDa one chain precursor enzyme into a 32/20-kDa two-chain mature and fully active form of CathA (Bonten & d'Azzo 2000). The mature form of CathA combines with two glycosidases, Neuraminidase-1 (NEU1), and β-Galactosidase (β-GAL) along with N-Acetylgalactosamine-6-sulfate sulfatase (GALNS), to form a LMC (Bonten et al. 2014). It has also been shown that GALNS play a role in the first step of the catalytic reaction of intralysosomal keratan sulfate. However, it is not clearly understood whether its activity directly relies on the interaction with other enzymes in the LMC (Pshezhetsky & Potier 1996). CathA is a member of the serine protease family of enzymes with carboxypeptidase activity at pHs from 4.5 to 5.5 and deamidase and esterase activity at pH 7.0. It has catalytic activity on vasoactive peptides, including angiotensin 1, bradykinin and endothelin-1, and neuropeptides such as substance P and oxytocin (van der Spoel et al. 1998) . Many studies showed that besides its catalytic role, CathA also activates and protects NEU1 and β-GAL against proteolytic degradation by the composition of a LMC. The complex is unable to form in the absence of CathA (Galjart et al. 1988). It has also been demonstrated that CathA functions in the regulation of the lysosomal pathway of protein degradation by inactivating the lysosome-associated membrane protein type 2a (lamp2a), a lysosomal integral membrane receptor protein involved in chaperone-mediated autophagy (Cuervo et al. 2003).

Sialic acids are monosaccharides which determine the chemical and biological structure and property of glycoconjugates. Sialic acid residues on glycan chains alter the localization of proteins, e.g. by targeting proteins to the lysosome for degradation. Sialidases (neuraminidases) are glycosidases which are located on the cell surface or in

4

intracellular compartments which function in the removal of α-glycosidically-linked sialic acid residues from glycan chains of glycoproteins and glycolipids (Miyagi & Yamaguchi 2012; Pshezhetsky & Hinek 2011). Studies characterizing sialidases introduced four types of mammalian sialidases as lysosomal NEU1, cytoplasmic NEU2, plasma membrane NEU3 and lysosomal/ mitochondrial NEU4 (Liang et al. 2006; Monti et al. 2010).

Structural analysis of binding sites on CathA and NEU1 demonstrated the formation of a heterodimeric complex between the two molecules. CathA is involved in the transportation of NEU1, as a chaperone protein, into the lysosomal compartment and it also plays a role in both the activation and stabilization/ maturation of NEU1 (Bonten et al. 2009)

NEU1 function within the lysosomes, as well as in the plasma membrane, makes it a critically key molecule for various physiological functions of the cell including lysosomal degradation of oligosaccharides, exocytosis, immune responses, elastic fiber assembly, generation of extracellular matrix, cell proliferation and cell differentiation via desialylation of specific protein targets (Miyagi & Yamaguchi 2012; Pshezhetsky & Hinek 2011). NEU1 deficiency is involved in two different neurodegenerative lysosomal storage disorders: sialidosis and galactosialidosis (Bonten et al. 1996; Pshezhetsky et al. 1997).

Deficiency of NEU1 leaves lysosomal associated membrane protein 1 (LAMP-1) hypersialylated which leads to accumulation of the protein at the cell membrane of hematopoietic cells, which is an indication of lysosomal exocytosis (Yogalingam et al. 2016). NEU1 also contributes to the production of Interferon gamma (IFNγ) in activated T lymphocytes (Nan et al. 2007).

A gene targeted mouse model of CathA$^{S190A-Neo}$ showed that reduced NEU1 activity results in increased sialylation of the cell surface proteins which suggests that desialylation of surface receptors through NEU1 activity regulates phagocytosis in macrophages and dendritic cells (Seyrantepe, Iannello, et al. 2010). NEU1 desialylation of α -2,3-sialyl residues of TLR receptors is essential for receptor activation and cellular signaling through NFkB activation in dendritic and macrophage cells (Amith et al. 2010). NEU1 acts on desialylation of microfibrillar glycoproteins and the deposition of insoluble elastin. NEU1 has a role in down regulation of smooth muscle cells by

desialylation of cell surface residing PDGF-BB and IGF-2 elastin receptors (Hinek et al. 2008). NEU1 can also play a role in muscle development and repair by desialylation of the insulin receptor, IGF-1, on skeletal myoblasts, which control the proliferative response of myoblasts to insulin (Arabkhari et al. 2010). Aberrant sialylation of molecules is highly associated with the malignant phenotypes of cancer cells including metastasis and invasiveness. An inverse relationship between NEU1 expression level and metastatic potential was shown in adenocarcinoma colon 26 cells and 3Y1 fibroblasts (Miyagi 2008). It has been shown that after overexpressing the human NEU1 gene into mice, liver metastasis was significantly reduced *in vivo*. *In vitro* analysis also indicated that cell migration, invasion and adhesion have negative correlations with NEU1 desialylation activity. NEU1 is important for integrin β4-mediated signaling in suppression of metastasis. Desialylation of β4 by NEU1 leads to decreased phosphorylation followed by reduction of the focal adhesion kinase (FAK) and extracellular signal regulated kinase 1/2 (ERK1/2) pathway and down-regulation of cell invasion and metastasis associated cancer matrix metalloproteinase-7 (Uemura et al. 2009). Promoting the growth of xenograft tumors by down-regulating three key pro-apoptotic and tumor suppressor genes makes miR-125b oncogenic in prostate cancer. Interestingly, NEU1 is one of the eight transcripts acting as metastatic suppressor which miR-125b targets (Shi et al. 2011).

In conclusion, various studies promote the novel role for NEU1 as an important enzyme modulating the activity of cell surface receptors. Disassociation of human NEU1 from LMC, consisting of CathA and β –GAL, results in sialidase inactivation and aberrations in many physiological activities (D'Azzo et al. 2001).

1.5 Lysosomal Disorders: Galactosialidosis, Sialidosis and GM1-Gangliosidosis

The enzymes in the LMC are ubiquitously but differentially expressed in different tissues and cell types, which provides for the independent and various roles of these enzymes in catalytic pathways even outside of the LMC. The genetic mutations on these enzymes is characterized by the occurrence of three lysosomal storage disorders:

Galactosialidosis (GS) (OMIM #256540), which is a deficiency of CathA accompanied by a secondary deficiency of NEU1 and β–GAL (de Geest et al. 2002); sialidosis, which is a direct deficiency of NEU1 (OMIM #256550) (Bonten et al. 2014); and GM1-gangliosidosis which occurs through lack of β–GAL (OMIM #230500, #23060, #230600) (Caciotti et al. 2011). Mutations in the CathA gene are the cause of the autosomally recessive lysosomal storage disorders. Lysosomal storage disorders are exemplified by a broad spectrum of clinical phenotypes from early-infantile severe forms to late infantile, juvenile/adult cases mostly associated with the age of onset and severity of their symptoms (Caciotti et al. 2013). The most severe form of the GS disease, the early infantile phenotype, presents with hydrop foetalis, inguinal hernia, macular cherry spots, visceromegaly, dysostosis multiplex, motor retardation, coarse facies, skeletal dysplasia and early death. The mild form of the disease, which is late infantile, is characterized with corneal clouding, cardiac involvement, visceromegaly and, rarely, psychomotor retardation. Symptoms are myoclonus, ataxia, seziure, progressive cognitive disability, neurological deterioration, angiokeratomas, absence of visceromegaly and longer survival than other disease forms (Caciotti et al. 2013).

Sialidosis and galactosialidosis patients have indistinguishable disease characteristics. Observed similarities in both diseases are expected because of the secondary deficiency of NEU1. Sialidosis is classified in two groups as type-I and type-II. Type-I or cherry-red spot myoclonus syndrome with gait disturbances, progressively reduced visual capacity, tremor, ataxia, seizures and no neurological signs is a less severe form of the diseases. However, type-II, which is also divided into two more classes based on age of onset, presents with more severe symptoms. Congenital sialidosis is a fulminant condition that develops before birth. Patients are either stillborn or die just after birth. Symptoms of juvenile/adult form of sialiodosis strongly resemble the severe symptoms of galactosialidosis. The typical feature of both GS and Sialidosis is gradually developing accumulation of sialylated glycoproteins and oligosaccharides in lysosomes of cells (D'Azzo et al. 2001).

GM1-gangliosidosis is a glycosphingolipid lysosomal storage disorder with clinical symptoms of mental retardation, motor activity decline, progressive loss in structure and function of neurons, and early death (Suziki et al. 2001). There are three forms of the disease known as infantile GM1 (type I), which is the most severe form,

the late infantile form (type II) and the last form is named as the chronic or adult GM1. G_{M1} accumulates in the brain and spinal cord of patients.

1.6   Animal Models

Mice models with homozygous deficiencies of CathA and NEU1 develop phenotypes with similar symptoms as characterized in human patients with early onset forms of the disease.

NEU1 knockout mice (NEU1$^{-/-}$) exhibit severe phenotypes closely resembling patients with type-II Sialidosis. After birth mice develop severe nephropathy, splenomegaly, kyphosis, edema of limbs, penis, eyelids and foreheads. They show weak appearance, loss of weight, enlarged kidneys, gait abnormalities, tremor, dyspnea Progressive deformity of the spine and lack of early degeneration of cerebellar Purkinje cells were further phenotypic features seen in NEU1$^{-/-}$ mice (de Geest et al. 2002).

CathA knockout mice (CathA$^{-/-}$) maintain a secondary deficiency of NEU1, however, the β –GAL activity is slightly affected in certain tissues of this mice model, which indicates that β–GAL has less dependency on a functional CathA enzyme in murine models. CathA knockout mice show splenomegaly, progressive nephropathy, ataxia and shortened life span. Therefore, cardiomyopathy and arterial hypertension which are commonly characterized symptoms in GS patients, might occur due to loss of CathA catalytic activity rather that loss of NEU1 and β–GAL (Zhou et al. 1995).

CathA knock-in (CathA^{S190A}) mice are a gene targeted mouse model in which a targeted point mutation in the *Ctsa* gene leads to a replacement in the CathA active catalytic site, Ser190, with Ala. Although CathA^{S190A} mice are fertile, show no developmental abnormality and have a normal life span, they have nearly zero CathA catalytic carboxypeptidase activity related with the Ser190Ala targeted mutation. On the other hand, western blotting and immunohistochemical staining showed normal levels of CathA protein as well as mRNA levels. In addition, biochemical analysis confirmed that sialidases in LMC showed normal enzyme activity in CathA^{S190A}. This inactive CathA is still able to form functional lysosomal multienzyme complexes, and as such

shows neither secondary deficiency of NEU1 nor β-GAL enzymes (Seyrantepe et al. 2008).

1.7 Peptides

CathA is active against various bioactive peptides; including endothelin-1, oxytocin and Substance P (Table 1.2.). Among the peptides studied, CathA has the highest relative activity against endothelin-1 (Hiraiwa 1999).

Table 1.2 Substrate specificity of CathA on bioactive peptide biology (adapted: Hiraiwa et al. 1999)

Peptide	Sequence	Relative activity (%)
Endothelin 1	Cys-Ser-Cys-Ser-Ser-Leu-Met-Asp-Lys-Glu-Cys-Val-Tyr-Phe-Cys-His-Leu-Asp-Ile-Ile-Trp-OH	100
Substance P	Arg-Pro-Lys-Pro-Gln-Gln-Phe-Phe-Gly-Leu-Met-NH$_2$	3.8
Oxytocin	Cys-Tyr-Ile-Gln-Asn-Cys-Pro-Leu-Gly-NH$_2$	4.0

1.7.1 Endothelin-1

Cys-Ser-Cys-Ser-Ser-Leu-Met-Asp-Lys-Glu-Cys-Val-Tyr-Phe-Cys-His-Leu-Asp-Ile-Ile-Trp-OH

Endothelin-1 (ET-1), which is a vasoconstrictor peptide, consists of a 21 amino acid sequence. By proteolytic cleavage of inactive pro-peptide ET-1 by a

metalloendopeptidase, ET-1 is converted into its active form (Xu et al. 1994). Inactivation of ET-1 occurs by degradation of its carboxyl terminus by CathA (Itoh et al. 2000).

ET-1 is an abundant peptide in the human cardiovascular system, the primary source of which is vascular endothelial cells (endothelium), in which also the highest level of CathA peptide is found (Yanagisawa et al. 1988; D'Azzo et al. 2001). Various cell types and organs are able to synthesize ET-1 such as epithelial cells, macrophages, monocytes, glial cells and neurons in the central nervous system and lungs and kidneys. (Davenport et al. 2016). In the brain, the cerebral cortex, striatum and hippocampus are the regions where ET-1 reactivity against anti- ET is most prevalent. Over stimulated ET-1 receptors on neurons may cause neuron death. Fibroblast cells from galactosialidosis patients, who are CathA deficient, revealed that these cells are unable to degrade endothelin-1 peptide (Itoh et al. 2000).

As ET-1 functions as a vasoconstrictor peptide, this could underlie its involvement in the pathogenesis of hypertension (Yanagisawa et al. 1988). Salt sensitive mice models of hypertension showed that vascular ET-1 amount is increased with a high salt diet. In addition to salt sensitive experiments, it has also been shown that endogenous infusion of ET-1 increases blood pressure in mice models (Davenport et al. 2016). Primary neural cells from CathA^{S190A} mice demonstrated significantly higher levels of ET-1. In addition to *in vitro* analysis, CathA^{S190A} mice and double deficient mice models of a CathA homolog, Scpep1$^{-/-}$/CathA^{S190A} have decreased ET-1 degradation rates in the blood plasma and lung tissues compared to their wild-type litter mates (Seyrantepe et al. 2008; Pan et al. 2014).

1.7.2 Oxytocin

Cys-Tyr-Ile-Gln-Asn-Cys-Pro-Lue-Gly-OH
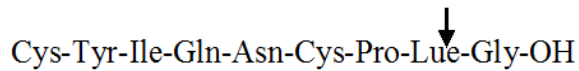
Oxytocin, which is a hypothalamic neuropeptide, consists of a 9 amino acid sequence. Oxytocin is synthesized in magnocellular and pervocellular neurons of paraventricular nucleus (Schulkin 1999). However, oxytocin receptors are expressed in the hippocampus (Vaccari et al. 1998; Breton & Zingg 1997), and oxytocin neurons of paraventricular nucleus send projections to hippocampus (Insel 1992; Schulkin 1999).

The primary role of the peptide is the regulation of mammalian social behavior and relationships such as pair bonding, aggression and social trust. In rodents, oxytocin modulates social recognition and fear conditioning, the sign of trust and avoidance behaviors respectively. Roles of oxytocin in social and fear behavior are directly related with effects of the peptide on specific brain areas, including the hippocampus for long term memory (Maroun & Wagner 2015). It has been reported that the hippocampal region of the brain is enriched with oxytocin receptors. It is also shown that oxytocin enhances the establishment of long term potentiation in the hippocampal CA1 region. Oxytocin administration in humans causes increased courage and trust behaviors; also intranasal administration of oxytocin in rat models leads to better spatial memory scores for treated animals and decreases the effects of stress conditioning on the related ERK pathway in the hippocampus (Kirsch 2005; Lee et al. 2015). Oxytocin induces spatial memory and long – lasting, long term potentiation in the hippocampus. However, oxytocin neither affects neurotransmission pre-synaptically or post-synaptically nor play role on phosphorylation of the GluR1 subunit of the AMPA receptor. In contrast, oxytocin enhancing long-term synaptic plasticity and improvement in the long term memory occurs via activation of the MAP kinase cascade and the consequent CREB phosphorylation in the hippocampus. Intracerebroventricularly oxytocin injected mice after eight-arm radial maze experiment showed the direct evidence for role of oxytocin on improvement of spatial learning and reference memory(Tomizawa et al. 2003).

1.7.3 Substance P

Arg-Pro-Lys-Pro-Gln-Gln-Phe-Phe-Gly-Leu-Met-OH
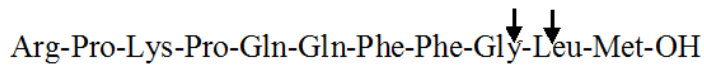
Substance P (SP), which is an endogenous neurokinin, consists of a 11 amino acid sequence. SP is localized to the central and peripheral nervous system where it is known to play a significant role in inflammation, blood pressure, anxiety, motor behavior, learning and memory. Numerous studies have pointed to the significance of SP in the hippocampus, where it has a primarily excitatory role (Yu et al. 2014).

1.8 Behavioral Tests

In order to evaluate behavioral differences in mice models, many test protocols have been introduced into cognitive science studies. The accelerating rotarod test is suitable for analyzing maximal motor coordination performance and possible motor coordination deficits. Passive avoidance tests assay fear based conditioned avoidance learning and memory in mice. The Morris water maze is sensitive in detecting spatial learning loss and memory dysfunction in rodents relying on distal cues to navigate towards an escape platform.

1.8.1 Rotarod Test

Motor coordination has traditionally been assessed in rodents by rotarod tests (Jones & Roberts 1968). The accelerating rotarod test uses a rotating horizontal rod that rotates about the long axis, onto which rodents are placed. The animal must walk forwards to remain upright and not fall off to the ground. The horizontal rotating rods force animals to use motor activity-related behaviors and allows evaluation of functional parameters such as balance, motor skills and coordination of the body in accordance with elapsed riding time and endurance (Piel et al. 2014).

1.8.2 Passive Avoidance Test

Learning experiments that have been precisely conducted for many years prove that conditioning stimulus promotes associations between an external stimuli and a response of subjects. Based on psychological learning theory, in the passive avoidance test, the animal which is being tested learns to suppress the instinctive "discover the area" response (a motor response) to stay away from the dark chamber which is associated with an aversive event. The dark compartment of the passive avoidance system is normally preferred over the brightly illuminated stressful compartment. The theoretical learning mechanism of passive avoidance test starts with an unconditional stimulus, which is a bright light chamber. The unconditional stimulus leads to conditioned adaptive behavioral response of fear after a brief foot shock (conditioned stimulus) in the dark chamber. The results of this learning experiment demonstrate the direct association between learning ability of the subject and the leaning center of the brain, the hippocampus (Ögren & Stiedl 2013).

1.8.3 Morris Water Maze Test

The Morris water maze is a behavioral tool used to test hippocampal-related learning and memory. The test is a widely accepted and highly applied protocol to assess spatial learning and memory functions in the study of neurobiology, neuropharmacology and neurocognitive disorders in rodent models (Morris 1981; Blokland et al. 2004). Some advantages of the Morris water maze over other methods of testing learning and memory are relatively shorter training time, no food restriction during the experiment, rapid learning of test parameters by subjects, control methods for distal cue learning and the absence of nonperformers. On the other hand, disadvantages include that this test may not be as sensitive for working memory, and some studies present concerns about stress inducing factors, however contrary evidences exists to refute this (Vorhees & Williams 2014).

Spatial memory protocols are applied in which the escape platform is placed at fixed locations into the pool relative to visual distal cues in the experiment room. The animals are placed into the pool facing towards the side of the pool from different starting positions each experimental day. They learn to swim to the escape platform with decreasing escape latencies and by choosing more direct paths with the help of visual distal cues hung around the sides of the room. A tracking software program supported by a video camera is used to measure parameters including path-length and swim speed (Sutherland et al. 1983).

After all training procedures are completed, a probe trial is applied, in which the submerged hidden escape platform is removed from the pool and the animals are allowed to swim for 60 seconds. A well-trained animal is expected to swim immediately towards to the target quadrant of the pool and spend more time here, looking for the removed platform repeatedly before searching elsewhere. Animals with defects in the hippocampus and dentate gyrus or combined physiological deficiencies score poorly in probe trials (Morris et al. 1982).

1.9 Aims

There are two main aims to this study. The first aim is to characterize the effects of CathA deficiency in the metabolism of vasoactive peptides. By using a mouse model in which the CathA enzyme activity has been abolished by a point mutation in the catalytic site (CathA^{S190A}), the effects of CathA inactivity on the distribution and accumulation of vasoactive peptides in the hippocampus region of the brain has been elucidated.

The second aim is to understand the impact of CathA deficiency on behaviour. By analyzing the performance of CathA^{S109A} mice in learning and memory-based tasks, the consequences of the downstream effects of a CathA enzyme deficiency has been investigated.
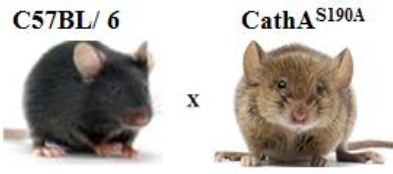
CHAPTER 2

MATERIALS AND METHODS

2.1.   Mouse Breeding

The CathA^{S190A} mouse model, which has a point mutation carrying a Ser190Ala replacement in the active site of the enzyme was generated by Prof. Dr. Volkan Seyrantepe during his post-doctoral studies and donated by Prof. Alexey V. Pshezhetsky (Centre Hospitaliere Universitaire Sainte- Justine, University of Montreal, Montreal, Quebec, Canada) (Seyrantepe et al. 2008). The mice with homozgous point mutations were bred with wild-type mice strain C57BL/6 to produce heterozygous females and males. Mice were further bred to produce homozygous colonies with point mutations and wild-type control littermates. Breeding pairs were selected between siblings to minimize genetic variation between animals, which could have otherwise emerged in the subsequent generations (Table 2.1). Only male mice were used for experiments.

Table 2.1 Breeding plan of CathA^{S190A}.

C57BL/ 6 x CathA^{S190A}	
F1 generation	
CathA$^{+/S190A}$ x CathA$^{+/ S190A}$	
F2 generation	
CathA$^{+/+}$ x CathA$^{+/+}$	CathA$^{S190A / S190A}$ x CathA$^{S190A / S190A}$

2.2.   Mouse Genotyping

Mice were genotyped from the genomic DNA extracted from tail. Tail tissue cut from mice were put in eppendorf tubes with 500 µl lysis buffer (consisting of 10% 1 M Tris pH 7.6, 2.5% 0.2 M EDTA, 20% SDS, 4% 5 M NaCl) and 12 µl Proteinase K (from 25 µg/µl solution). Samples were incubated in an incubator shaker at 55˚C at 70 rpm overnight. The next day samples were centrifuged at 14,000 rpm for 10 minutes. Supernatants were transfered into new 1.5 ml- eppendorf tubes and 500 µl 100% isopropanol was added into the tubes. DNA was collected and transferred into a new eppendorf containing 70% ethanol. After 1 minute centrifugation at 14,000 rpm, supernatant was removed and the remaining ethanol was completely air dried for 10 minutes. DNA was dissolved in 200 µl ultra pure water and incubated at 55˚C for 1 hour. Concentrations of DNA were measured with a Nanodrop spectrophotometer (ND-1000). The PCR for CathA^{S190A} and control groups were performed with 100 ng genomic DNA in the 25 µl reaction mix containing 50 pmol of each primer, 10 mM of dNTPs, 1.5 units Taq polymerase (New England Biolab), 1.5 mM MgCl$_2$, 10 mM Tris-HCl and 50 mM KCl buffer containing 10% DMSO. Allele specific primers for wild-type and mutant alleles were used for detection of CathA^{S190A} and control groups (Table 2.2). Conditions for PCR were 1 cycle 30 seconds at 95˚C; 30 cycles 30 seconds at 95˚C, 45 seconds at 60˚C, 45 seconds at 72˚C; and 1 cycle 5 minutes at 72˚C. The PCR for CathA^{S190A} was performed with 100 ng genomic DNA in the 50 µl reaction mix containing 50 pmol of each primer, 10 mM of dNTPs, 2.5 units Taq polymerase, 1.5 mM MgCl2, 10 mM Tris-HCl and 50 mM KCl buffer. A primer set pair was used to amplify the CathA^{S190A} and wild-type alleles (Table 2.2). Conditions for PCR were: 1 cycle 5 minutes seconds at 92˚C; 30 cycles 45 seconds at 92˚C, 45 seconds at 57˚C, 45 seconds at 72˚C; and 1 cycle 5 minutes at 72˚C. As the CathA^{S190A} allele has an NdeI enzyme recognition site, the genotype of CathA^{S190A} allele was revealed after digestion of the PCR product in a 20 µl reaction mix containing 20 units NdeI (New England Biolabs) enzyme in 1X buffer, incubated overnight at 37˚C.

Table 2.2 Sequences of primer set used in genotyping.

Gene	Primer Name	Primer sequence
CathA^{S190A}	ScreenF	GGTGGCGGAGAACAATTATG
	ScreenR	AACAGAAGTGGCACCCTGAC

2.3. Immunohistochemistry

Fixed tissues were prepared for immunohistochemical analysis by transcardiac perfusion of CathA^{S190A} mice and their wild-type siblings. Sodium pentobarbital and ketamine/xylazine were administered as anesthetic agents. Responsiveness to tail and toe pinches was assessed. The mouse was immobilized lying on its back in a face upward position by taping the hindpaws and forepaws to the work place in a fume hood. An incision was made through the skin with surgical scissors along the thoracic midline from just under the xiphoid process to the clavicle. The diaphragm was separated from the chest with scissor cuts. The reflected ribcage was taped to expose the heart. The beating heart was secured with the help of forceps. Immediately, the needle was inserted in the left ventricle. No damage occured to the beating heart. The needle was secured to the base of the left ventricle. The right atrium was cut by scissors and as the first sign of blood flow was observed, 0.9% NACl buffer (pH 7.4) was infused to organs. The process was continued until the fluid exiting the right atrium was completely clear. NaCl perfusate was switched to 4% freshly prepared paraformaldehyde fixative. Approximately, 20-30 ml of fixative was applied according to size of the animal. Having a stiff, whip-like tail was used as a good indicator of a successful fixation of entire organs. The mouse was decapitated by large surgical scissors and the brain tissue was carefully collected. Cervical dislocation often damages the caudal brain structure. The collected brain samples were incubated in 4% paraformaldehyde solution at 4°C for 16 hours. Samples were incubated in 10% and 20% sucrose in 0.2 M Phosphate Buffer Saline (PBS, pH 7, 6) at room temprature for 2 hours respectively, and incubated in 30% sucrose in 0.2 M Phosphate Buffer Saline (TBS, pH 7, 6) at 4°C for 16 hours. Brain samples were then embedded with OCT (optimal cutting temperature) into

cryomolds standing with olfactory bulbs facing upwards. Cryomolds were incubated in styrofoam buckets filled with dry ice for 30 minutes until the whole brain sample was frozen. Tissues were placed into -80°C for later use. The temperature of the cryostat chamber (Leica CM1850UV) was set to - 20°C. The tissue was placed in the chamber of the cryostat and the temperature allowed to equilibrate for at least 30 minutes. Ten-twelve micron thick sections were coronally sectioned and collected onto gelatin-coated slides at -20°C. Tissue sections were stored at -80°C, unless they immediately were used for further immunostaining procedure (Schneider Gasser et al. 2006; Risher et al. 2014).

2.3.1. Vectastain ABC Method

The sections were air dried and then fixed with 4 % paraformaldehyde for 30 minutes. Slides were then transferred into PBS buffer before incubation in 0.3% H2O2 in methanol for 30 minutes. Following a five minute wash in buffer, the slides were incubated for 20 minutes with diluted normal blocking serum, which was prepared from the species of which the secondary antibody was derived. Excess serum was blotted from slides. Slides were then incubated for 30 minutes with primary antibody diluted in buffer and then washed for 5 minutes in buffer. They were then incubated for 30 minutes with diluted biotinylated secondary antibody solution before washing for 5 minutes in buffer. Sections were then incubated for 30 minutes with VECTASTAIN® ABC Reagent and again washed for 5 minutes in buffer. Slides were lastly incubated in peroxidase substrate solution until the desired stain intensity developed, rinsed in tap water, and counterstained by haematoxylin and mounted.

VECTASTAIN ELITE ABC kit was applied for this study. The same primary antibodies which were applied in immunofluorescence were applied for this protocol (Table 2.3.).

2.3.2. Immunofluorescence

Sections with similar sizes of the hippocampal region from CathA^{S190A} mice and their wild-type siblings were washed for 5 minutes in PBS three times at room temperature. Sections were then incubated in cold acetone for 15 minutes before being washed for 5 minutes in PBS three times at room temperature. Sections were blocked in 5% Normal Goat Serum (NGS) in TBST for 1 hour at room temperature. Primary antibodies (rabbit anti-Endothelin 1:750 [ab113697, ABCAM], rabbit anti-oxytocin 1:500 [ab 2078, ABCAM], guinea pig anti-SubstanceP 1:500 [ab1053, ABCAM]) were diluted in 5% NGS containing PBS. Sections were incubated overnight at 4°C with primary antibodies. Secondary Alexa-fluorophore conjugated antibodies (ABCAM) were added (1:500 in PBS with 5% NGS) for 2 hr at room temperature. Slides were mounted with DAPI (ab104139, ABCAM) and images were acquired and quantified on an OLYPUS BX53 fluorescence microscope (Table 2.3.).

Table 2.3 Primary and secondary antibodies applied in immunofluorescence

Primary Antibody	Dilution Ratio	Catalog Number	Secondary Antibody	Dilution Ratio	Catalog Number
rabbit anti-Endothelin	1:750	ab113697, ABCAM	Anti-rabbit IgG AlexaFluor 488	1:500	Ab150077 ABCAM
rabbit anti-oxytocin	1:500	ab 2078, ABCAM	Anti-rabbit IgG AlexaFluor 488	1:500	Ab150077 ABCAM
guinea pig anti-SubstanceP	1:500	ab1053, ABCAM	Goat Anti-Guinea pig IgG HL AlexaFluor 488	1:500	Ab150185 ABCAM
DAPI	-	ab104139, ABCAM		2 drops	

2.4.   Behavioral Analysis

In this study, we applied three behavioral tests to assess differences between genotypes and age groups of CathA^{S190A} mice and wild-type littermates. The rotarod test was used to assess differences in motor coordination and performance. passive avoidance test to evaluate alterations in learning and memory, and the Morris water maze test was used to investigate consolidation and reconsolidation of spatial memory formation and distal cue oriented learning abilities.

2.4.1. Rotarod Test

The rotating rod motor coordination test was performed using an accelerating Rota-rod treadmill (Panlab, Harvard Apparatus) for mice (3 cm diameter and 30 cm above the base of the apparatus) to assess for motor deficits. Animal were transferred into the test room 30 minutes prior to the experiment. Animals were briefly trained before the test at 4 rpm on a 5 line rotarod unit. 10 seconds after placing the mouse on the rod, acceleration was started (the subject was facing forward), and the speed at which the mouse fell off was noted. The animals that jumped or rejected standing over the rod were removed from the experiment. The rotarod was set with a start speed of 4 rpm, acceleration rate 40 rpm/minute .The animals were then tested using an accelerated mode from 4 to 40 rpm over 5 minutes. Three trials were performed per day. Each trial was separated by a 20 minute rest period. The length of time that each animal was able to stay on the rod was recorded. Data was analyzed by Sedacom v 2.0 software (Harvard Apparatus).

2.4.2. Passive Avoidance Test

The passive avoidance test consists of three different trials for 3 consecutive days, which are a habituation trial, a training trial and a test trial. In the habituation trial, a certain time is given for the animal to discover the experiment conditions. In the training day, the animal receives a mild foot-shock to establish conditioned fear. In the test day, mice memory and learning functions are assessed based on their decision whether or not to re-enter the dark box, where previously they received the foot-shock.

2.4.2.1. Habituation Trial

On the habituation day, the subject was placed into the illuminated compartment facing the guillotine door while the door that separates dark and light chambers was closed. After 30 seconds the guillotine door was automatically opened and the mouse was allowed 5 minutes to explore both chambers. Each trial began with the presentation of 80 lux light conditioned stimuli into the chamber where the mouse was located. The latency to enter into the dark compartment was recorded. After the animal stepped into the dark compartment with all four paws, the door was closed automatically. The animal was allowed 10 seconds for the complete exploration of the dark chamber. The animal was removed from the dark compartment through the backdoor of the dark compartment. The mouse was placed back into its home cage.

2.4.2.2. Training Trial

On the training day (24 hours after habituation trial), the subject was placed into the light compartment under the same conditions as the habituation day, except the automatic guillotine door was opened from the beginning of the experiment. The latency to enter the dark compartment was recorded. When the animal stepped into the dark compartment with all four paws, the door was closed and a 1-2 second footshock was delivered (0.2 mA shock). The animal remained in the dark compartment for an

additional 10 seconds after the termination of the aversive stimuli, before being removed and placed back into its home cage. The apparatus was cleaned with 70% ethanol in between animals.

2.4.2.3. Test Trial

On the test day (24 hour after training trial), the animal was placed inside the white compartment and the door was raised to allow access to the dark compartment. The latency to re-enter the dark compartment was recorded, however, there was no aversive stimulus applied to the animal upon re-entry into the dark compartment during testing. Shut Avoid Vol 1.8 HARVARD APPARATUS was used during the experiment.

2.4.3. Morris Water Maze

The Morris Water Maze Test (MWM) was used to evaluate spatial learning and memory. The CathA^{S190A} mice and their wild-type siblings were placed into a circular pool with a diameter of 140 cm and depth of 45 cm. As black animals were used during the experiment, a white pool was used. The room in which the experiment was conducted was precisely isolated from all possible distracting visual clues for the animals during experiments. The room also was arranged in such a way that the animal being tested was not able to see the experimenter from the pool. Spatial clues with a height of 80 cm and width of 45 cm and with different high contrast patterns were placed on walls of the room in north, south, east, and west directions. A white platform, with height of 34 cm and diameter of 6 cm was located in different fixed locations on each day, and was used as an escape platform for mice inside the pool. The platform was kept visible by keeping it 2 cm above the water level on the first three days, and was made invisible on the last 5 days of the experiment by keeping it submerged 2 cm below the water level. 300 g milk powder was added into the pool and mixed thoroughly each day before starting the experiment in order to make the inside of the pool and the platform invisible for mice during swimming session. The water and the

room temperature were kept to 19°C during the experiment. The mice used in the experiment were transferred from their housing facility to the experiment room within their cages half an hour before the experiment began. Mice were kept in an area where they could not see the pool or the spatial cues, and allowed to become adapted to the new room/ environment for at least 30 min before the experiment. Swimming patterns of animals were automatically recorded by using a Sony SSC- G18 model camera centrally positioned above the water tank. Behavioral differences were analyzed by using PENLAB SMART Video Tracking System V 0.3 (Harvard Apparatus). The mice were given three trials per day using three different starting positions assigned in fixed order between randomly chosen subjects. At the end of each day the water was drained and the empty pool was cleaned carefully (Seyrantepe, Lema, et al. 2010; Blokland et al. 2004)

2.4.3.1. Day 1-3: Visible Platform

In the first three-day trial, a colorful flag was used to allow the mice to detect the placement of the platform easily. The platform was placed in the same quadrant (in the middle of south and east directions) while starting positions and swimming orders of mice changed each day. If the subject did not find the platform within 60 seconds, it was guided to the platform and helped to climb onto the platform. The subject was left on the platform for 10 s to discover visual clues and the platform. If they were able to find the platform before 60 s, elapsed time stopped and the subject was allowed to stay on the platform for 5 s before returning to its cage. On each of the three days mice were placed into the pool from three different directions, and the order of the directions was altered each day.

2.4.3.2. Day 4-8: Hidden Platform

The platform was submerged under the water level and placed in different quadrants on each day. Visual clues were reoriented to ensure the platform was placed between the same two visual clues as during the first three days. This allows the

experimenter to disregard subjects using an unrelated clue inside of the room to find its way to the platform on the first three days, instead of the visual clues. 90 s was given to each animal to find the hidden platform. Unsuccessful animals were helped to the platform and given 10 s on the platform for observation. Mice performed three trials each day from different directions.

2.4.3.3.   Probe Trial

The platform was removed from the pool. The probe trial was given two hours after the last trial on the eighth day. 60 s was given to all mice to searched the zone where previously the platform was located, from three different directions.

2.4.4.   Statistical Analysis

All data were processed and analyzed using Excel (Microsoft) software. Quantification of accumulation of the peptides in hippocampal areas was performed using FIJI software (Schindelin et al. 2012). Statistical differences between wild-type animals and $CathA^{S190A}$ were tested by t-test. Statistical analyses with respect to genotype in the same age group of animals for rotarod and passive avoidance experiments were tested by t-test. Quantification and analysis of water maze data was recorded using the video- track system as previously described. For each acquisition trial the latency (i.e., time in seconds spent by mice before reaching the platform), moved distance to the platform and proximity of the animal's position with respect to the goal was measured. Potential group differences with respect to age and genotype were tested by factorial ANOVA.

CHAPTER 3

RESULTS

3.1. Mice Genotyping

Littermates were genotyped for the presence of the CathA^{S190A} allele (Figure 3.1) and mated with each other to obtain animals homozygous for the CathA^{S190A} allele.
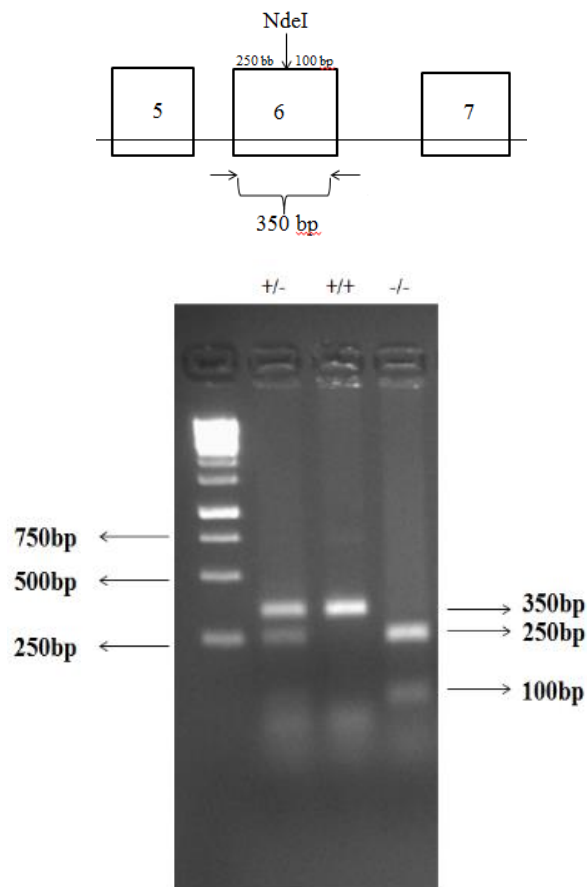

Figure 3.1 Gel image of *Nde I* digested PCR amplification of CathA gene with primers. Screen F and Screen R generated a 250- bp fragment in wild-type mice, 250 – and 350- bp fragments in heterozygous CathA^{S190A} mice and a 350-bp fragment in homozygous CathA^{S190A} mice.

3.2. The Distribution of Vasoactive Peptides is Altered in the CathA^{S190A} Mouse Hippocampus

To determine the effect of CathA inactivation on neuropeptide and vasoactive biology, the distribution of these peptides in the brain tissue of CathA^{S190A} mice was compared to their wild-type littermates. Tissues were analysed from mice at 3, 6 and 12 months of age, using primary antibodies detected by either biotin- or fluorescently-tagged secondary antibodies. Images shown are from the hippocampal region of the brain, which is fundamentally essential to learning and memory and in which CathA is thought to play a role.

3.2.1. Endothelin-1

To characterize the distribution and accumulation level of vasoactive endothelin-1 peptide, mouse brain tissues were stained with both haemotoxylin and anti-endothelin-1 antibody detected using a biotin-tagged secondary antibody (Figure 3.2). These images demonstrate several findings. Firstly, is that the gross morphology of the hippocampus is unaltered in CathA^{S190A} mice compared to their wild-type littermates, as seen by the similarities between the haemotoxylin staining (which identifies cell nuclei) between the two genotypes. Secondly, is that there is differential accumulation of endothelin-1 between the two mouse genotypes.

In 3-month-old animals (Figure 3.2A) an increased staining throughout the CA1-CA3 regions of the hippocampus was detected in the CathA^{S190A} animals compared to their wild-type littermates, consisting of punctate regions of accumulated endothelin-1 peptide. At 6- and 12-months-old (Figure 3.2.B & C respectively), the increase in staining seen is more diffuse, and the patchy punctate regions seen at 3 months can no longer be observed.

These finding were further examined using a second method of detection. Instead of using a secondary antibody conjugated to biotin, a fluorescently-tagged antibody was used (Figures 3.3-3.8).

Figure 3.3 shows the hippocampi of 3-month-old wild-type and CathA^{S109A} mice. Quantification of fluorescent intensity shows that significant increased accumulation of endothelin-1 can be observed in the hippocampal region of CathA^{S190A} mice brains compared with their wild-type littermates, $p < 0.05$, (Figure 3.4A). Staining in the CathA^{S190A} brains is both spread more widely throughout the hippocampus and is more intense suggesting that a lack of CathA activity leads to an accumulation of full-length endothelin-1 and diffusion throughout the hippocampus. The CA1, CA2 and CA3 regions of the hippocampus are the regions most affected by the CathA activity deficiency in 3-month-old animals (Figure 3.4).

Figure 3.5 shows endothelin-1 staining in the hippocampus of 6-month-old animals, again in combination with DAPI staining. The quantification results show significantly increased endothelin-1 staining seen in the wild-type animals' whole hippocampus when compared to the 6-month-old wild-type animals, $p < 0.05$, (Figure 3.6). Despite this, once again there is increased staining of endothelin-1 in CathA^{S190A} animals, and again this staining is both more intense and more diffuse. In these animals, the CA1, CA2 and CA3 regions of the hippocampus are the most affected by deficiency of CathA. There is a significant accumulation of endothelin-1 in the CA3 region (Figure 3.6D).

At 12 months of age (Figure 3.7), endothelin-1 can be detected in the wild-type animals, but in the CathA^{S190A} animals much more widely diffused staining throughout the whole hippocampus was observed. Total accumulation of endothelin-1 in the whole hippocampus in CathA^{S190A} animals was significantly higher than wild-type littermates, $p < 0.05$, (Figure 3.8). The accumulation pattern was dense in CA1 and CA2 regions, yet there is no significant change in the CA3 region (Figure 3.8B, 3.8C, 3.8D).

WT   CathA^{S190A}

A.

B.

C.
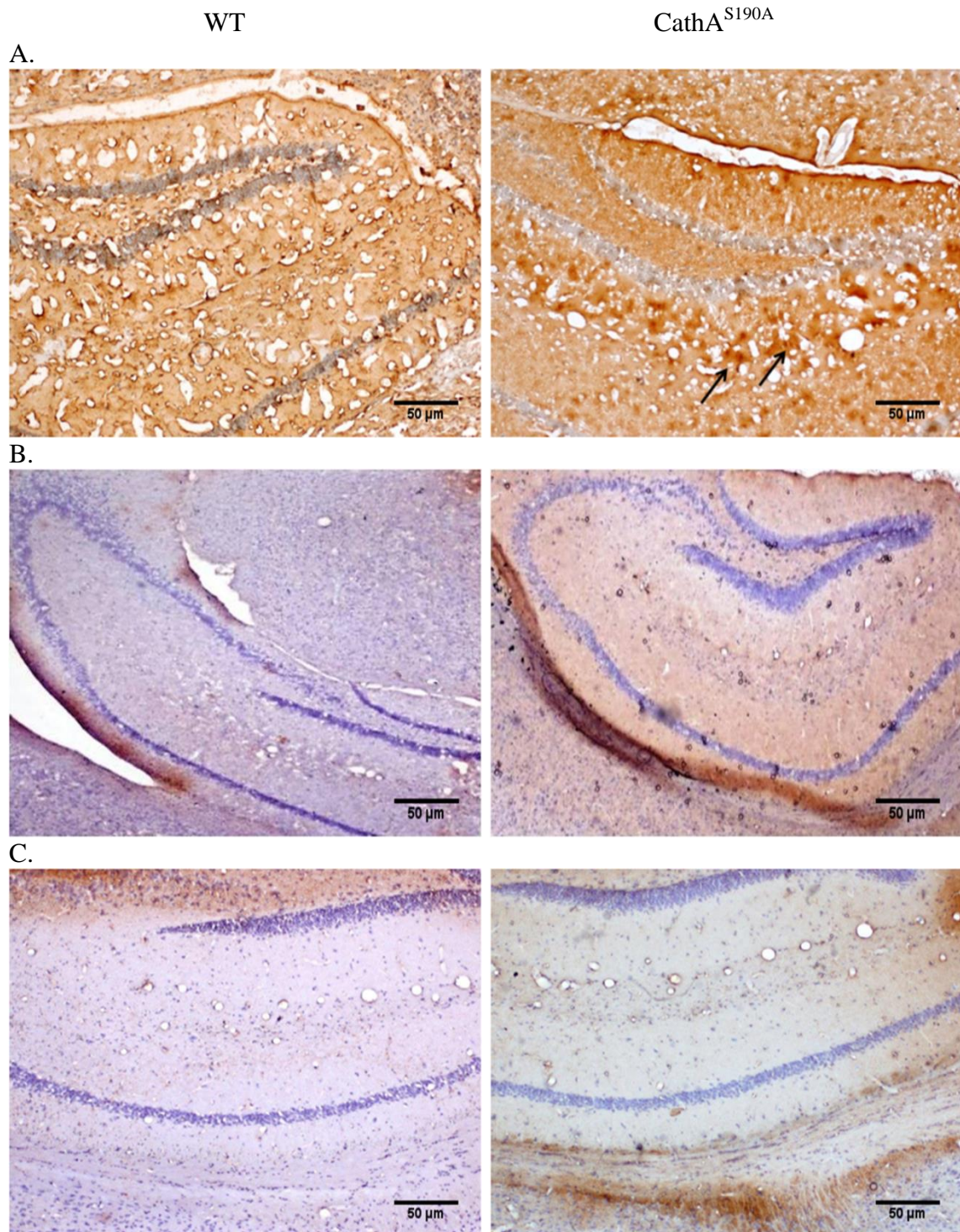
Figure 3.2 Distribution of Endothelin-1 in the hippocampus of wild-type and CathA^{S190A}
        mice. Representative images showing the hippocampi of wild-type and
        CathA^{S190A} animals after staining with Endothelin-1 antibody and
        haemotoxylin at 3-months-old (A), 6-months-old (B) and 12-months-old
        (C). Images were taken at 20 x magnification; n=3. No cells were labeled
        when the primary antibody was omitted.

WT   CathA^{S190A}

A.

B.

C.

Figure 3.3 Hippocampal endothelin-1 distribution in 3-month-old CathA^{S190A} mice and wild-type littermates. Images show the hippocampi of 3-month-old wild-type littermates and CathA^{S190A} animals after staining with Endothelin-1 antibody and DAPI. 3 animals are shown per genotype. A. Animal 1; B Animal 2; C. Animal 3. Images were taken at 20 x magnification. No cells were labeled when the primary antibody was omitted.

Figure 3.4 Quantification of hippocampal endothelin-1 distribution in 3-month-old CathA^{S190A} mice and wild-type littermates. Graphs show the region-specific accumulation comparison of endothelin-1 in hippocampi. 6 hippocampi from 3 different animals per genotype were analyzed. A. Total fluorescence intensity in hippocampus; B. CA1 region-specific endothelin-1 accumulation; C. CA2 region-specific endothelin-1 accumulation; D. CA3 region-specific endothelin-1 accumulation. Graph shows average fluorescence intensity ± standard error of the mean.

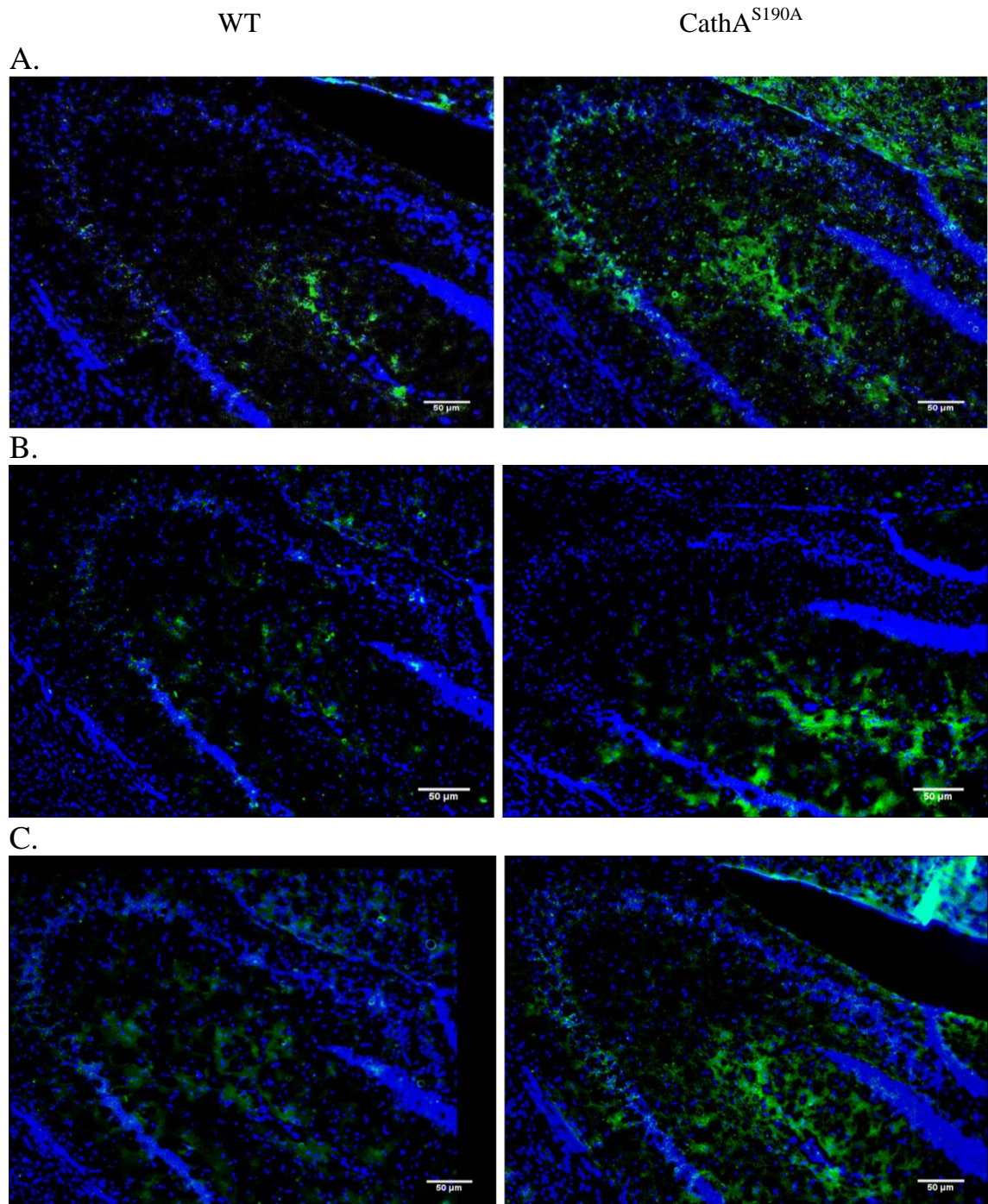WT   CathA^{S190A}

A.

B.

C.

Figure 3.5 Hippocampal endothelin-1 distribution in 6-month-old CathA^{S190A} mice and wild-type littermates. Images show the hippocampi of 6-month-old wild-type and CathA^{S190A} animals after staining with Endothelin-1 antibody and DAPI. 3 animals are shown per genotype. A. Animal 1; B Animal 2; C. Animal 3. Images were taken at 20 x magnification. No cells were labeled when the primary antibody was omitted.
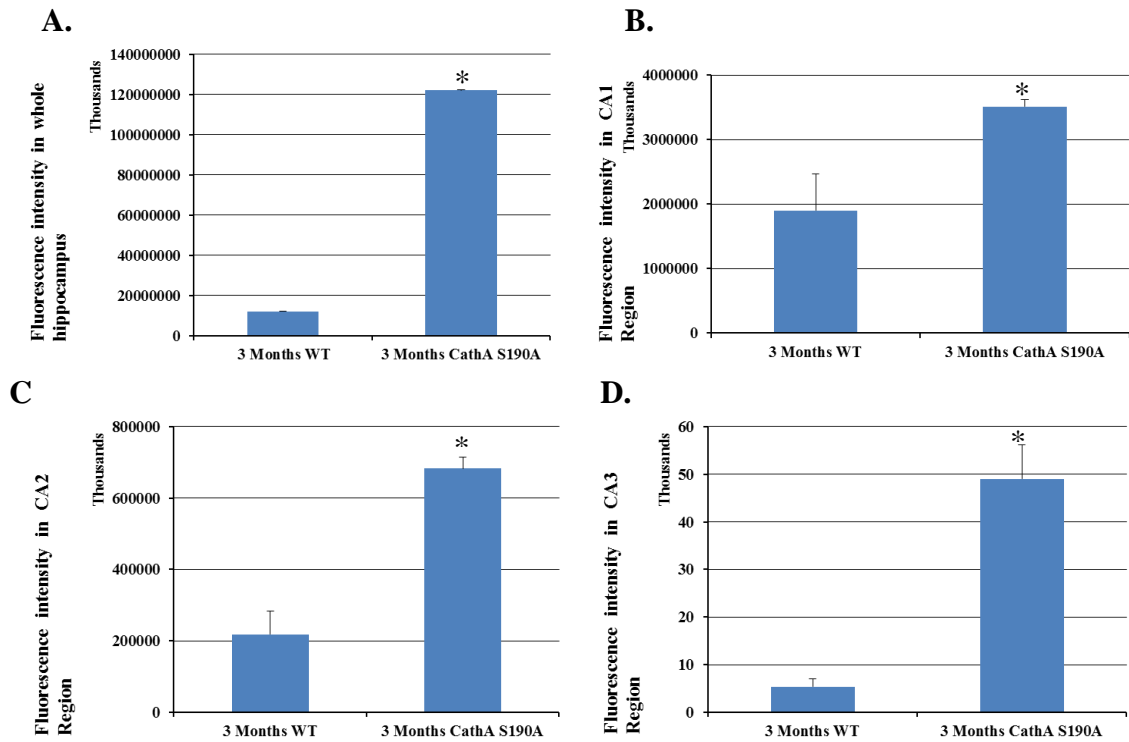
Figure 3.6 Quantification of hippocampal endothelin-1 distribution in 6-month-old CathA^{S190A} mice and wild-type littermates. Graphs show the region-specific accumulation comparison of endothelin-1 in hippocampi. 6 hippocampi from 3 different animals per genotype were analyzed. A. Total fluorescence intensity in hippocampus; B. CA1 region-specific endothelin-1 accumulation; C. CA2 region-specific endothelin-1 accumulation; D. CA3 region-specific endothelin-1 accumulation. Graph shows average fluorescence intensity ± standard error of the mean.
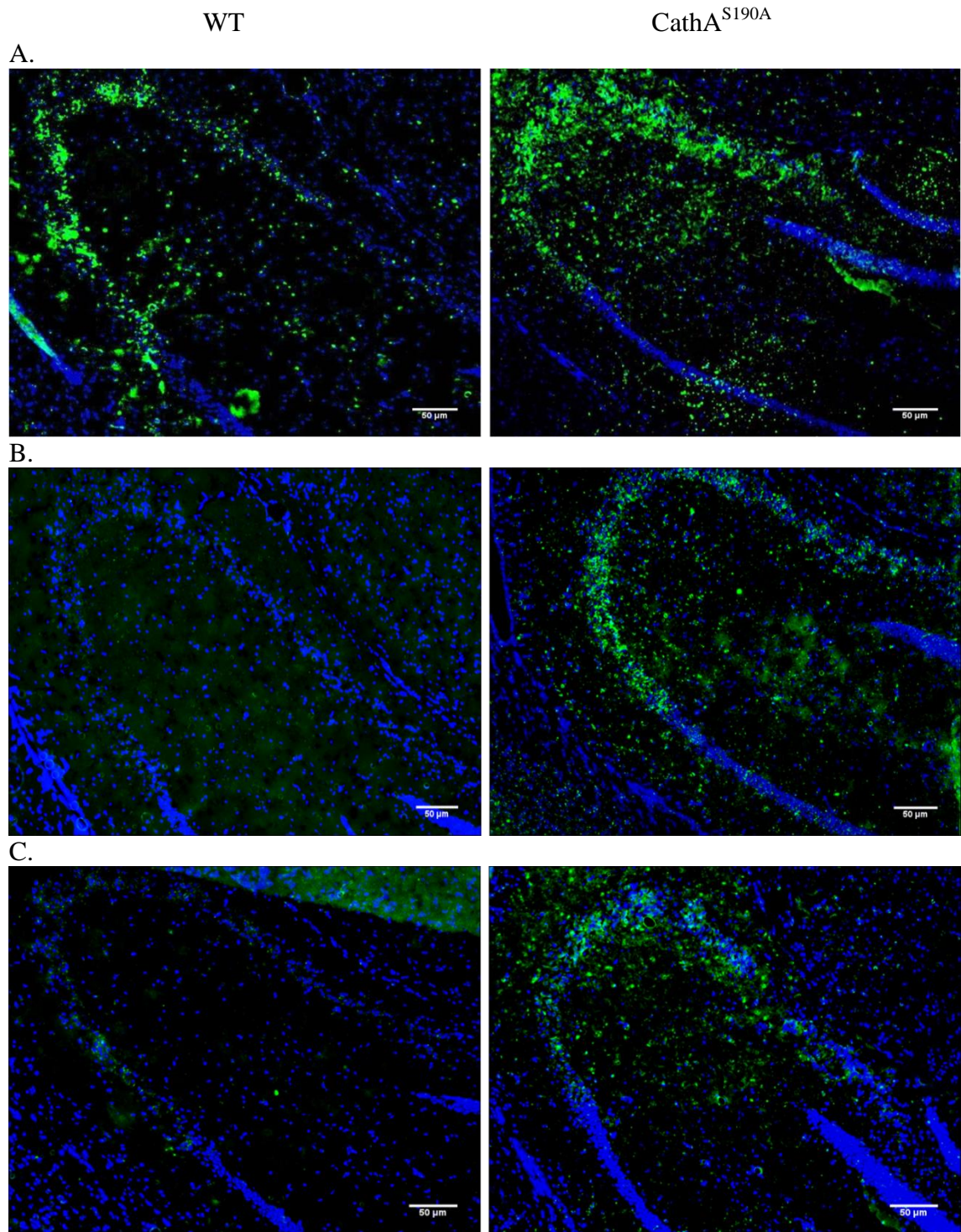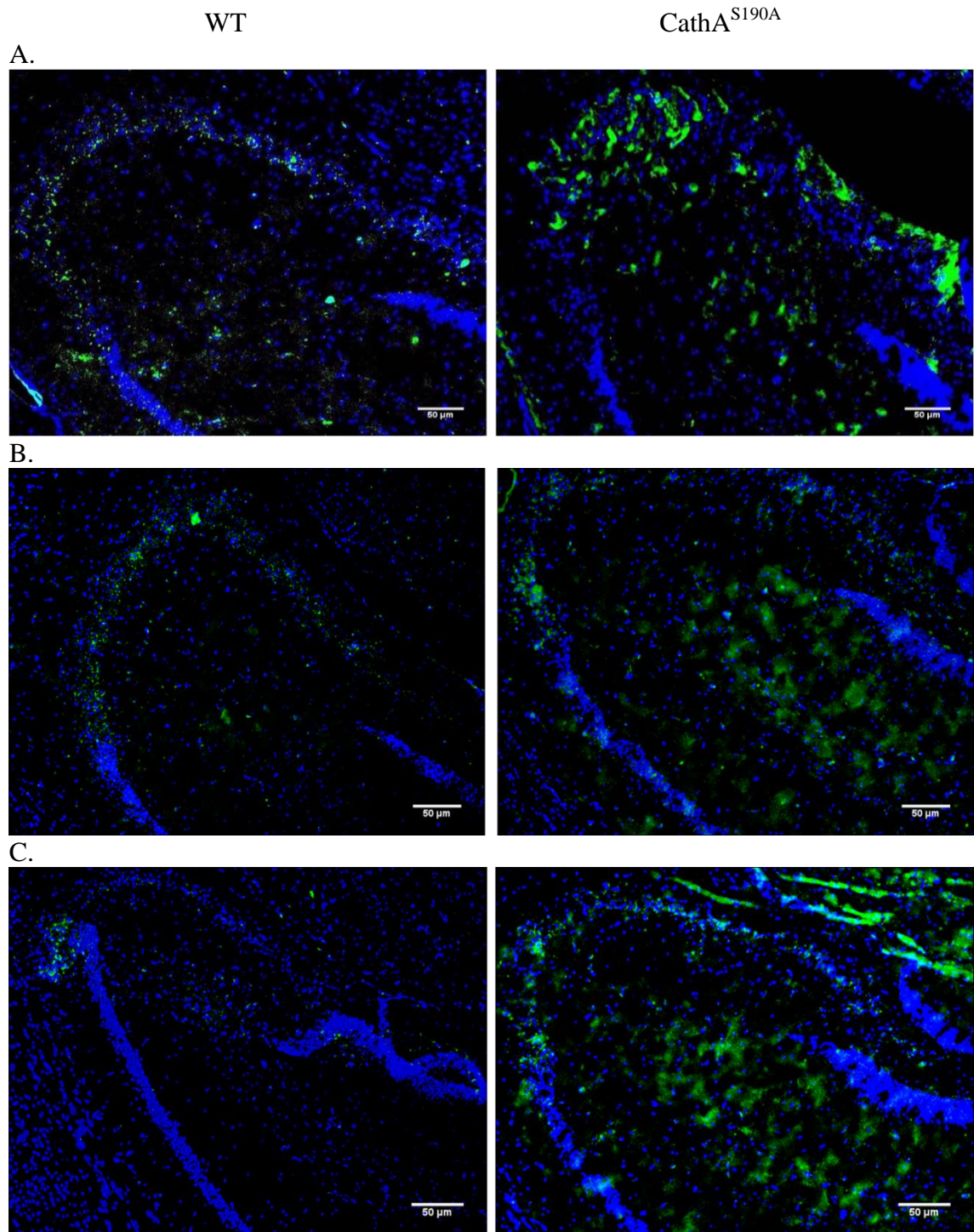
WT   CathA^{S190A}

Figure 3.7 Hippocampal endothelin-1 distribution in 12 month old CathA^{S190A} mice and wild-type littermates. Images show the hippocampi of 12 month old wild-type littermates and CathA^{S190A} animals after staining with Endothelin-1 antibody and DAPI. 3 animals are shown per genotype. A. Animal 1; B Animal 2; C. Animal 3. Images were taken at 20 x magnification. No cells were labeled when the primary antibody was omitted.
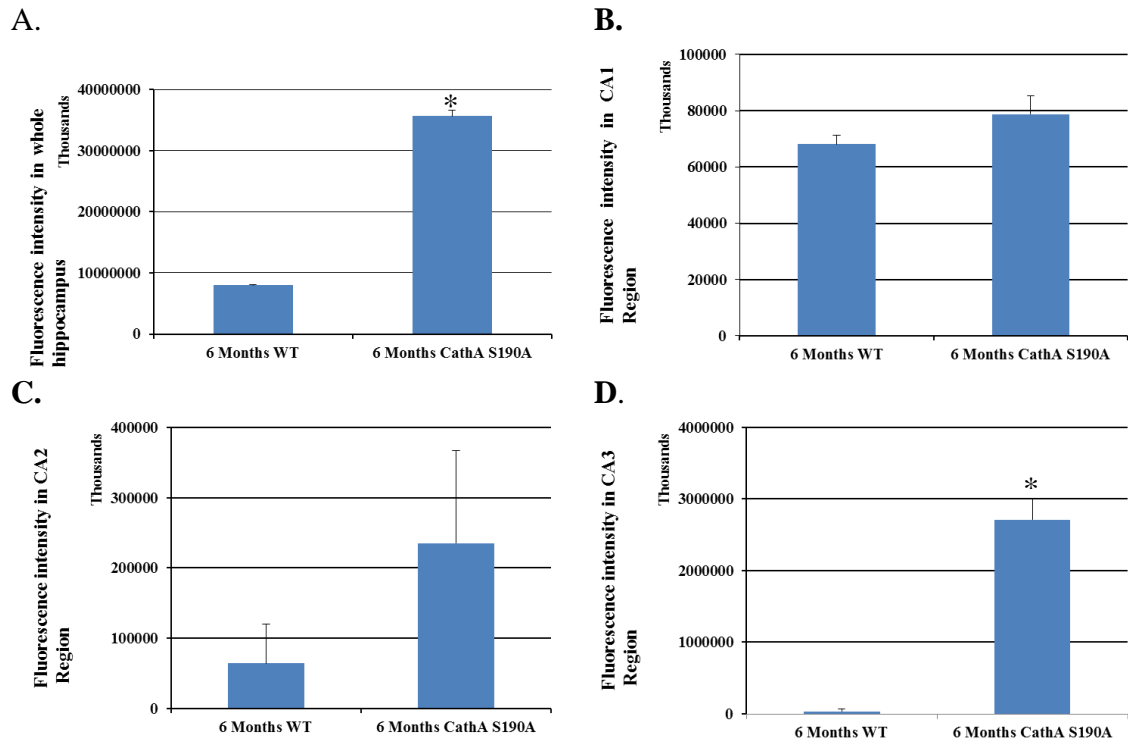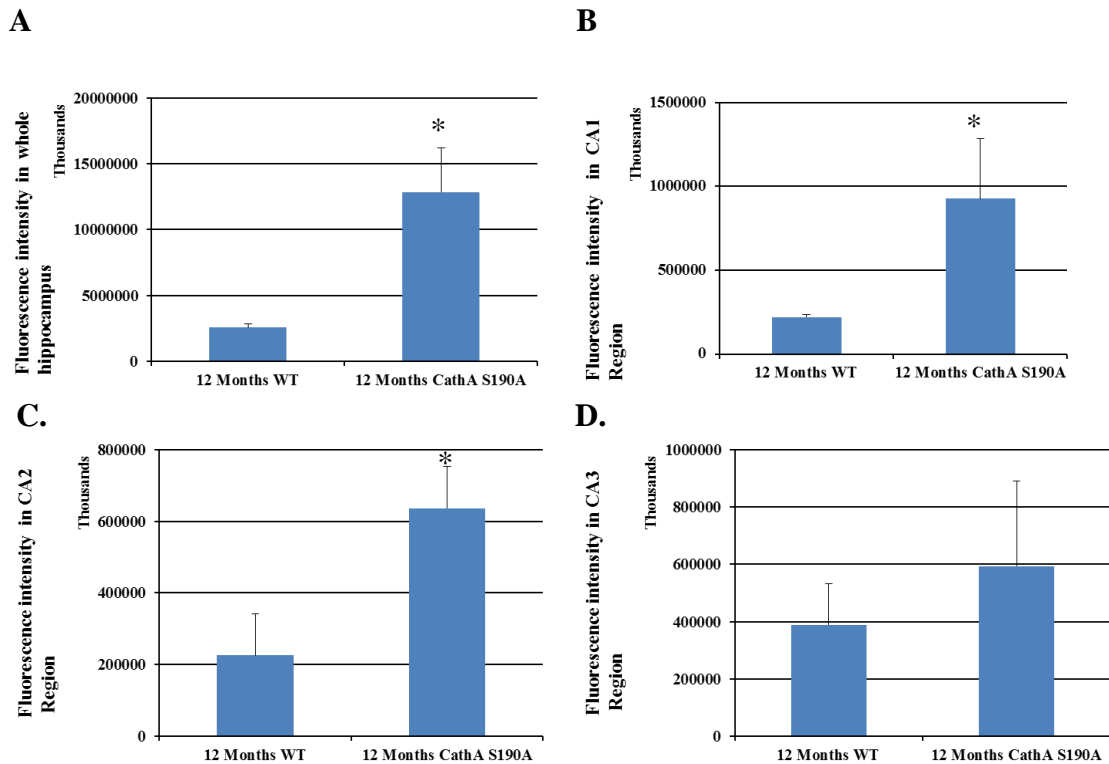
Figure 3.8 Quantification of hippocampal endothelin-1 distribution in 12-month-old CathA^{S190A} mice and wild-type littermates. Graphs show the region-specific accumulation comparison of endothelin-1 in hippocampi. 6 hippocampi from 3 different animals per genotype were analyzed. A. Total fluorescence intensity in hippocampus; B. CA1 region-specific endothelin-1 accumulation; C. CA2 region-specific endothelin-1 accumulation; D. CA3 region-specific endothelin-1 accumulation. Graph shows average fluorescence intensity ± standard error of the mean.

3.2.2. Oxytocin

Oxytocin is a vasoactive peptide metabolized by CathA that functions physiologically in the regulation of social behaviour. To characterize the accumulation level of Oxytocin peptide in animals with an inactive CathA enzyme, 3-, 6- and 12-month old mice brain tissues were stained with an antibody against Oxytocin (Figures 3.9-3.14).

Figure 3.9 shows oxytocin in the hippocampi of wild-type and CathA^{S190A} animals detected using a biotin-conjugated secondary antibody. In 3-month-old animals (Figure 3.9A), there is increased staining in the CA1-CA2 regions of the hippocampi of

CathA^{S190A} mice. There are also relatively large patches of oxytocin staining in this region. This increase is maintained in the 6-month-old and 12-month-old animals (Figure 3.9B & C respectively), but by 12 months, large diffuse patches of accumulated peptide can be seen scattered across the hippocampus.

Figure 3.10 shows oxytocin staining in the hippocampi of CathA^{S190A} mice and their wild-type littermates at 3-months-old, detected using a fluorescently-tagged secondary antibody. Similarly to endothelin-1 staining, a signficant increase is seen in whole hippocampus staining in the CathA^{S190A} animals, $p < 0,05$, (Figure 3.11A). In these animals there is a strong accumulation of the full-length oxytocin peptide in a band running from CA1-CA3, a pattern that is not seen for the endothelin-1 peptide (Figure 3.11B, 3.11D).

At 6 months (Figure 3.12) there is an increased amount of oxytocin in both the wild-type and CathA^{S190A} mice hippocampi compared to mice at 3 months. Significantly increased, $p < 0,05$, oxytocin staining can be seen in the hippocampus of CathA^{S190A} mice when compared to their wild-type littermates, however the tight band of increased staining seen in 3-month-old animals has largely dissipated. Instead, the peptide accumulation is more diffuse throughout the entire hippocampu (Figure 3.13).

Figure 3.14 shows oxytocin staining in the brains of 12-month-old wild-type and CathA^{S190A} mice. The increase in oxytocin staining in CathA^{S190A} animals at this age is much less ordered. In these brain slices, diffuse patches of accumulated oxytocin are spread throughout the hippocampus. Whilst oxytocin staining can be seen in wild-type brains, the puncta of peptide are much smaller with more defined edges. A significant increase in accumulation of oxytocin in the whole hippocampus and CA1, CA2 and CA3 regions of CathA^{S190A} hippocampus is seen when compared with wild-type littermates, $p < 0,05$, (Figure 3.15).

WT CathA^{S190A}

A.

B.

C.
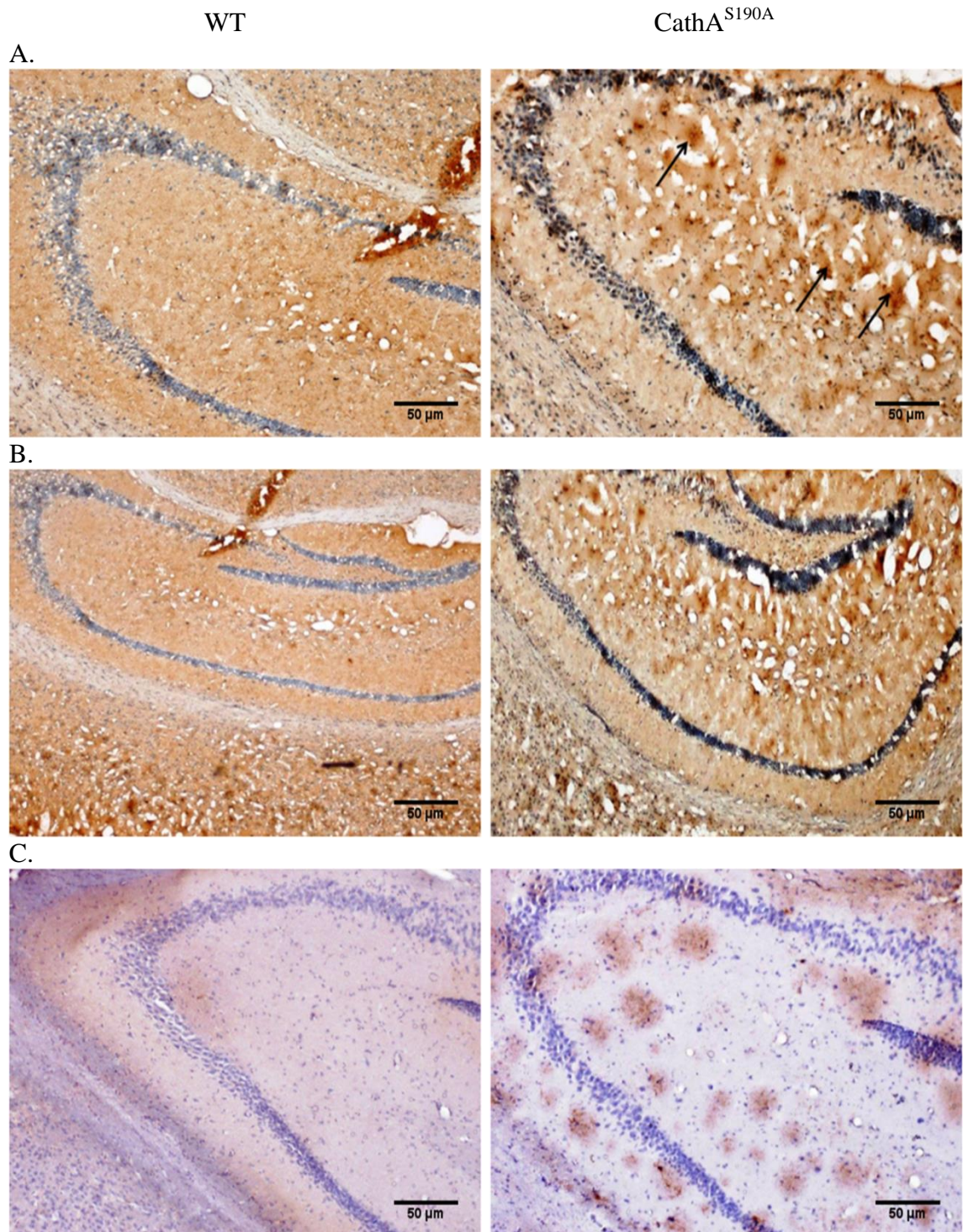
Figure 3.9 Distribution of oxytocin in the hippocampus of wild-type and CathA^{S190A} mice. Representative images showing the hippocampi of wild-type and CathA^{S190A} animals after staining with oxytocin antibody and haemotoxylin at 3-months-old (A), 6-months-old (B) and 12-months-old (C). Images were taken at 20 x magnification; n=3. No cells were labeled when the primary antibody was omitted.

36

Figure 3.10 Hippocampal oxytocin distribution in 3-month-old CathA^{S190A} mice and wild-type littermates. Images show the hippocampi of 3-month-old wild-type littermates and CathA^{S190A} animals after staining with oxytocin antibody and DAPI. 3 animals are shown per genotype. A. Animal 1; B Animal 2; C. Animal 3. Images were taken at 20 x magnification. No cells were labeled when the primary antibody was omitted.

Figure 3.11 Quantification of hippocampal oxytocin distribution in 3-month-old CathA^{S190A} mice and wild-type littermates. Graphs show the region-specific accumulation comparison of oxytocin in hippocampi. 6 hippocampi from 3 different animals per genotype were analyzed. A. Total fluorescence intensity in hippocampus; B. CA1 region-specific oxytocin accumulation; C. CA2 region-specific oxytocin accumulation; D. CA3 region-specific oxytocin accumulation. Graph shows average fluorescence intensity ± standard error of the mean.

WT   CathA^{S190A}

A.

B.

C.
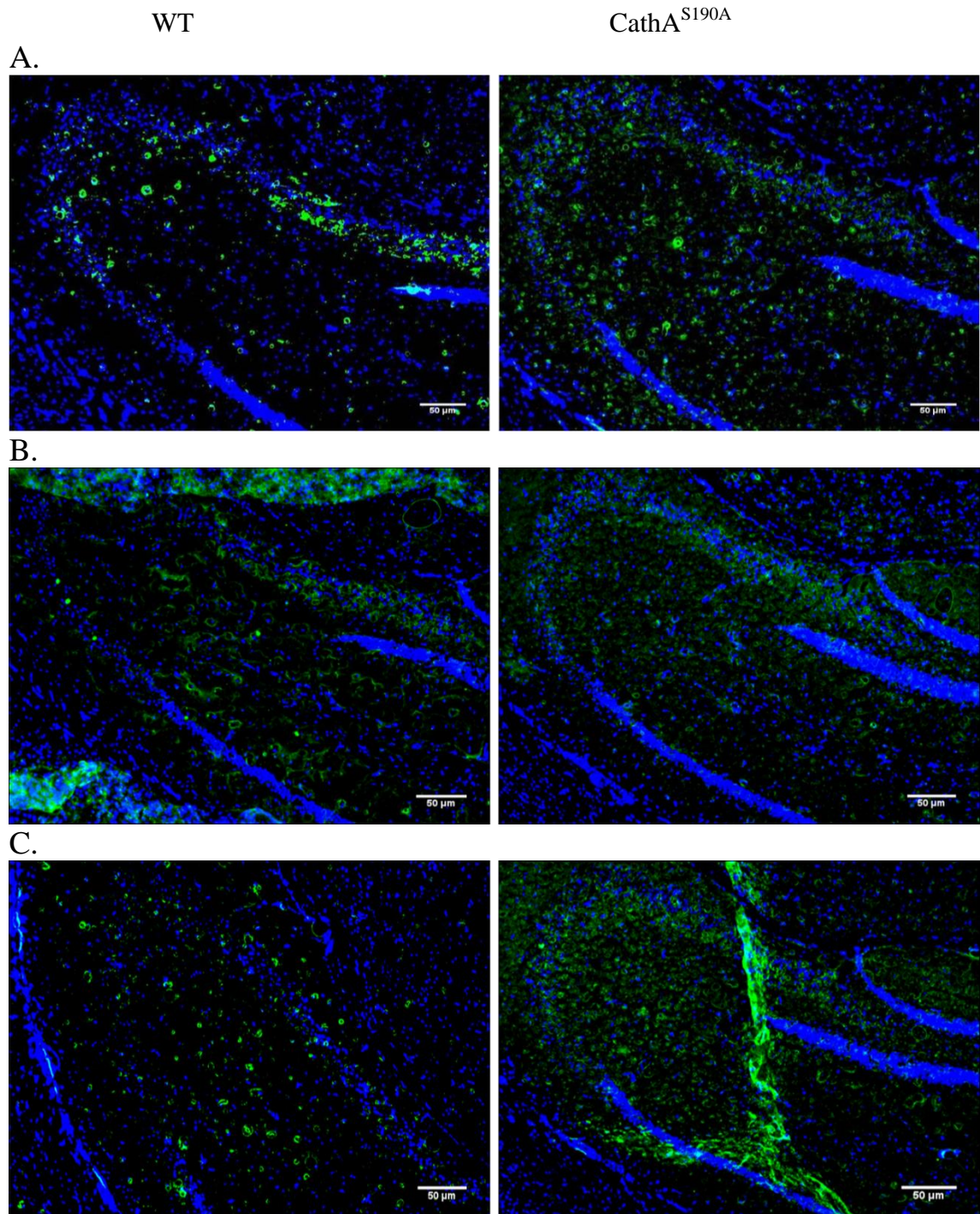
Figure 3.12 Hippocampal oxytocin distribution in 6-month-old CathA^{S190A} mice and wild-type littermates. Images show the hippocampi of 6-month-old wild-type littermates and CathA^{S190A} animals after staining with oxytocin antibody and DAPI. 3 animals are shown per genotype. A. Animal 1; B Animal 2; C. Animal 3. Images were taken at 20 x magnification. No cells were labeled when the primary antibody was omitted.
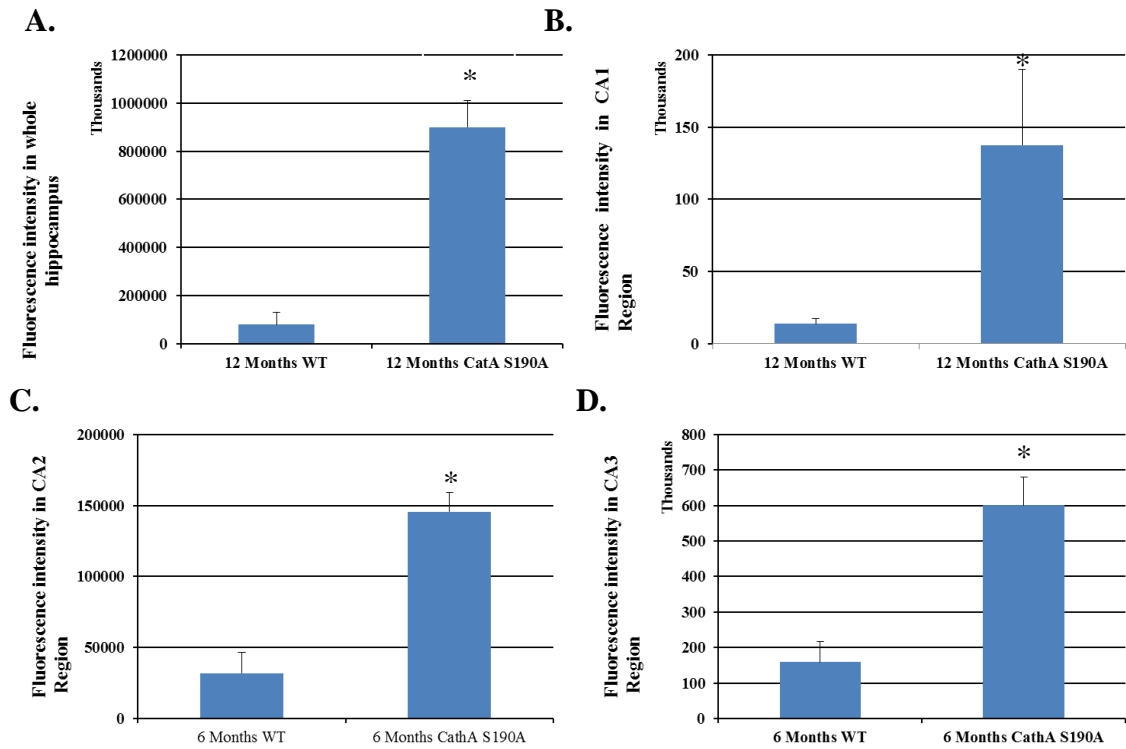
Figure 3.13 Quantification of hippocampal oxytocin distribution in 6-month-old CathA[S190A] mice and wild-type littermates. Graphs show the region-specific accumulation comparison of oxytocin in hippocampi. 6 hippocampi from 3 different animals per genotype were analyzed. A. Total fluorescence intensity in hippocampus; B. CA1 region-specific oxytocin accumulation; C. CA2 region-specific oxytocin accumulation; D. CA3 region-specific oxytocin accumulation. Graph shows average fluorescence intensity ± standard error of the mean.
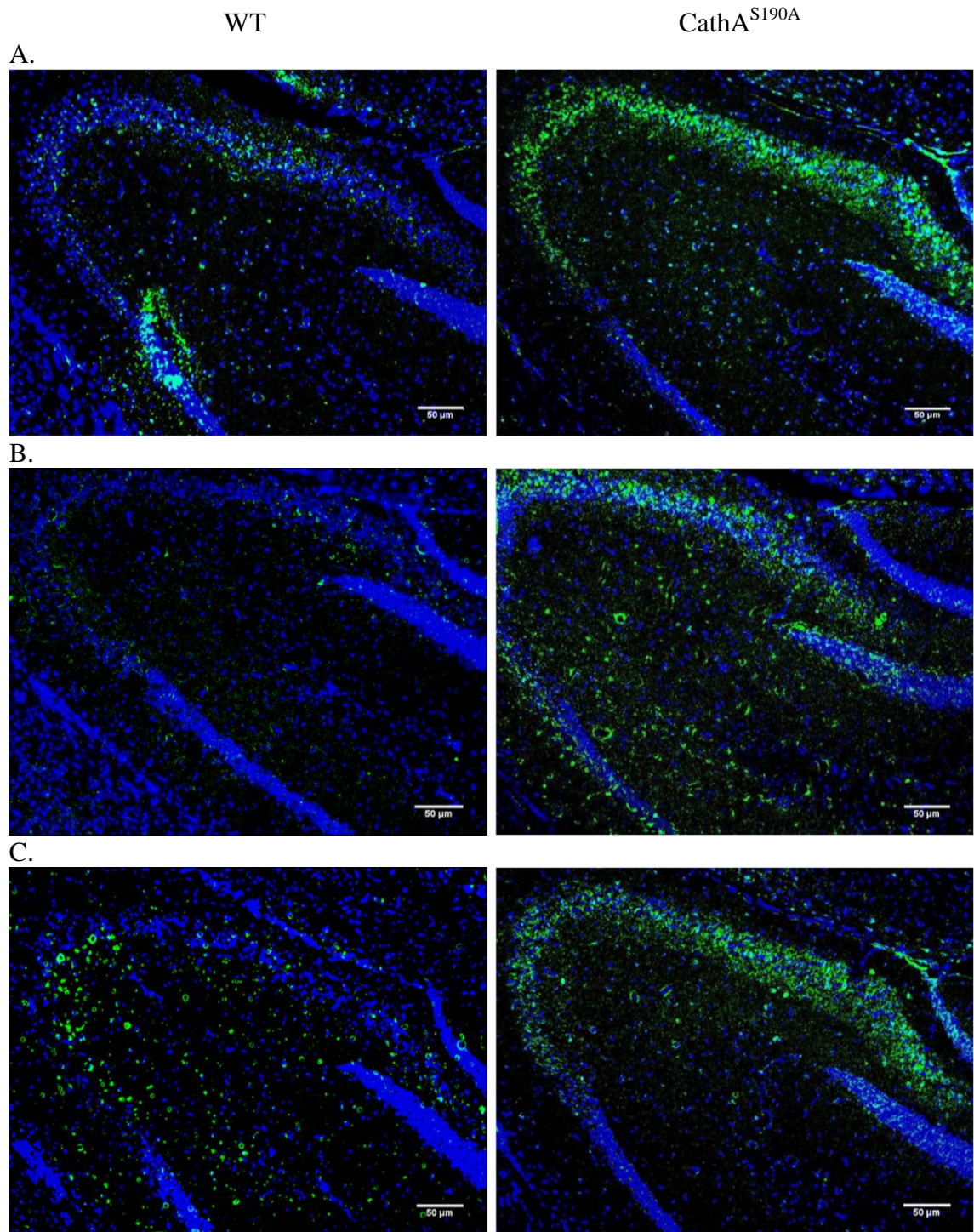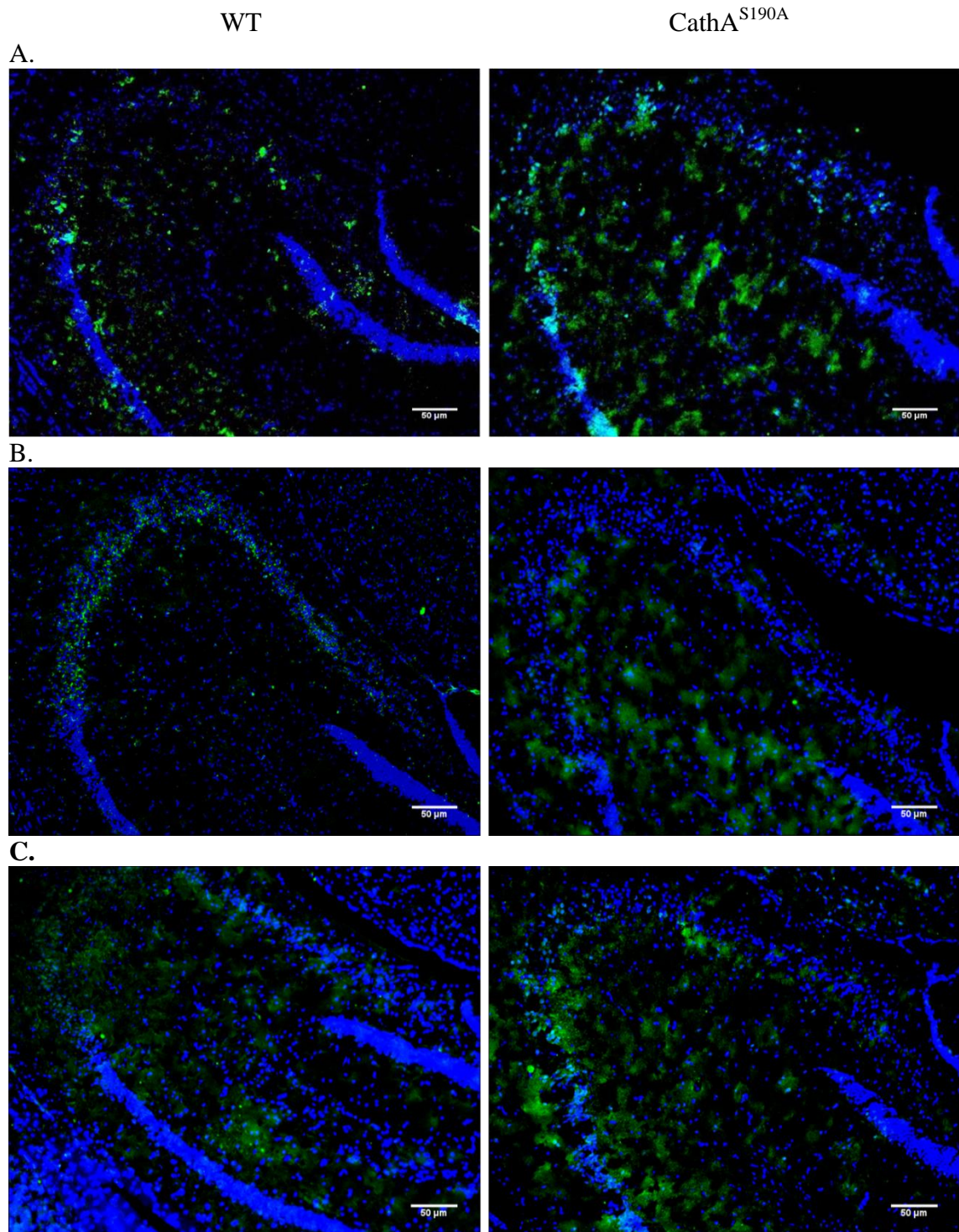
Figure 3.14 Hippocampal oxytocin distribution in 12-month-old CathA^{S190A} mice and wild-type littermates. Images show the hippocampi of 12-month-old wild-type littermates and CathA^{S190A} animals after staining with oxytocin antibody and DAPI. 3 animals are shown per genotype. A. Animal 1; B Animal 2; C. Animal 3. Images were taken at 20 x magnification. No cells were labeled when the primary antibody was omitted.
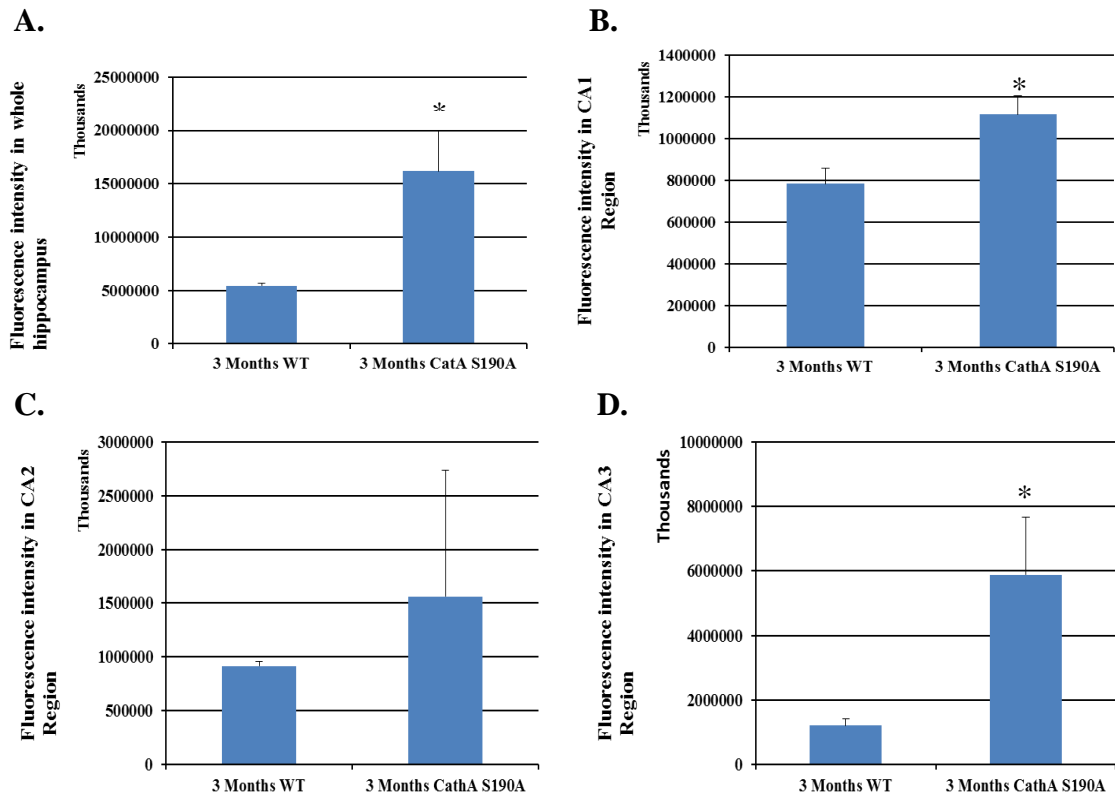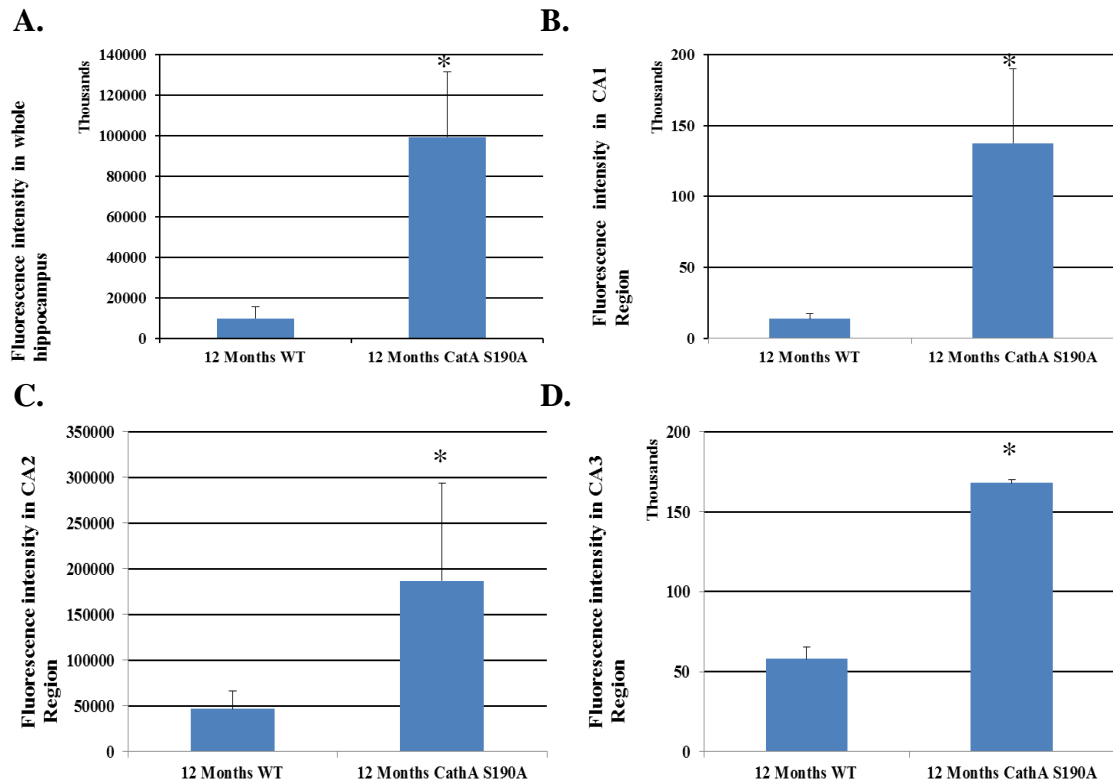
Figure 3.15 Quantification of hippocampal oxytocin distribution in 12-month-old CathA^{S190A} mice and wild-type littermates. Graphs show the region-specific accumulation comparison of oxytocin in hippocampi. 6 hippocampi from 3 different animals per genotype were analyzed. A. Total fluorescence intensity in hippocampus; B. CA1 region-specific oxytocin accumulation; C. CA2 region-specific oxytocin accumulation; D. CA3 region-specific oxytocin accumulation. Graph shows average fluorescence intensity ± standard error of the mean.

3.2.3. Substance P

To characterize the accumulation level of vasoactive Substance P peptide, 3-, 6- and 12- month old mice brain tissues were stained with anti-Substance P antibody (Figures 3.16-3.19). Figure 3.16 shows hippocampi of both wild-type and CathA^{S190A-} mice stained with a Substance P antibody detected by a biotin-conjugated secondary antibody. These images show a strong band of peptide staining in the CathA^{S190A} mouse cortex (indicated by arrow) that is not present in their wild-type littermates. This band is more intense in older mice, and becomes more diffuse.

Figures 3.17-3.19 show staining of Substance P in the hippocampus of wild-type and CathA^{S190A} mice, using a secondary conjugated to a fluorophore instead of biotin. These figures, which show slices from 3-month-old (Figure 3.17), 6-month-old (Figure 3.18) and 12-month-old (Figure 3.19) animals, do not show any differences in staining between the two genotypes. Despite a deficiency in the activity of CathA, there seems to be no accumulation of Substance P in the hippocampus of these mice.

WT CathA^S190A

A.

B.

C.
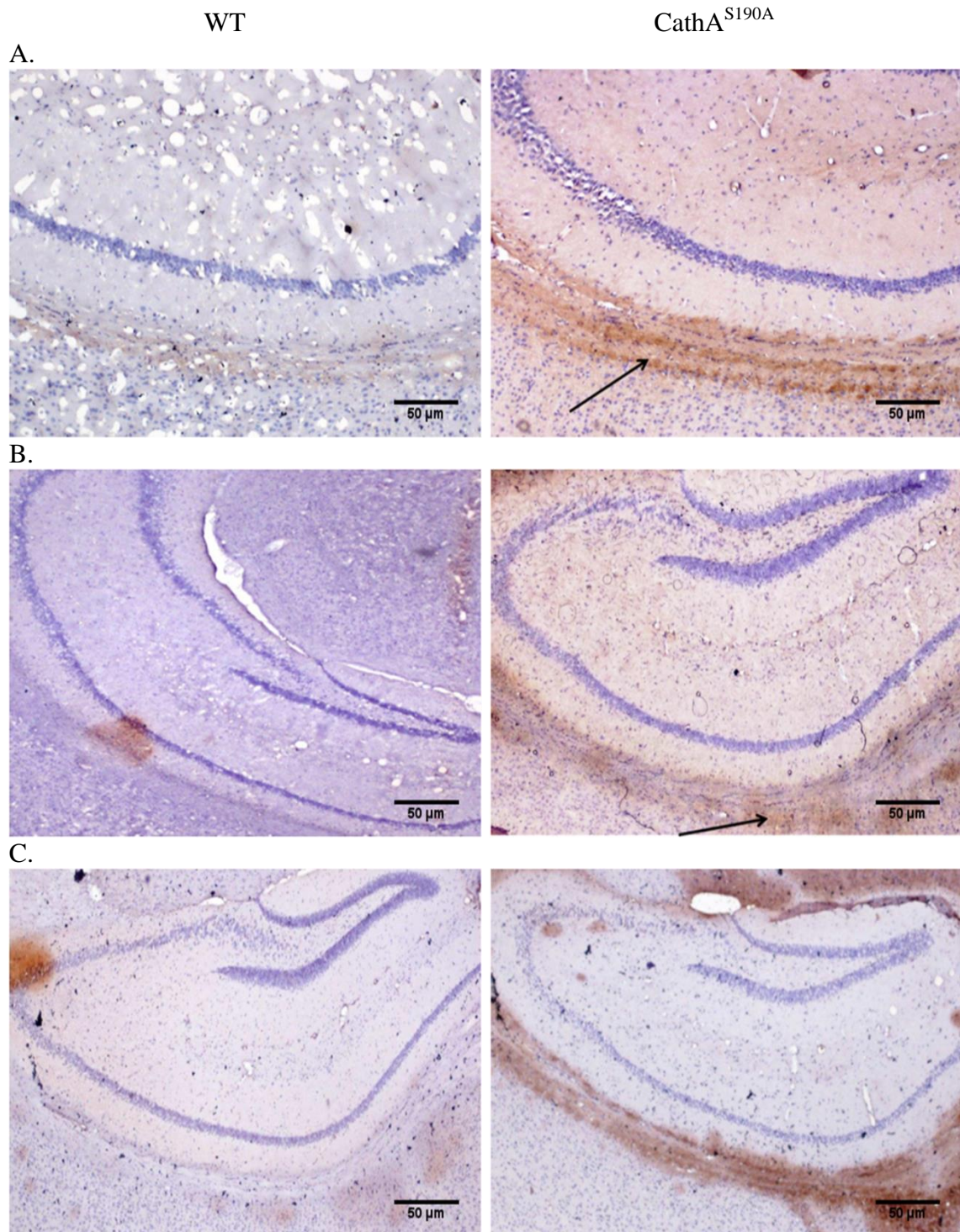
Figure 3.16 Distribution of Substance P in the hippocampus of wild-type and CathA^S190A mice. Representative images showing the hippocampi of wild-type and CathA^S190A animals after staining with Substance P antibody and haemotoxylin at 3-months-old (A), 6-months-old (B) and 12-months-old (C). Images were taken at 20 x magnification; n=3. No cells were labeled when the primary antibody was omitted.

WT   CathA^{S190A}

A.

B.

C.
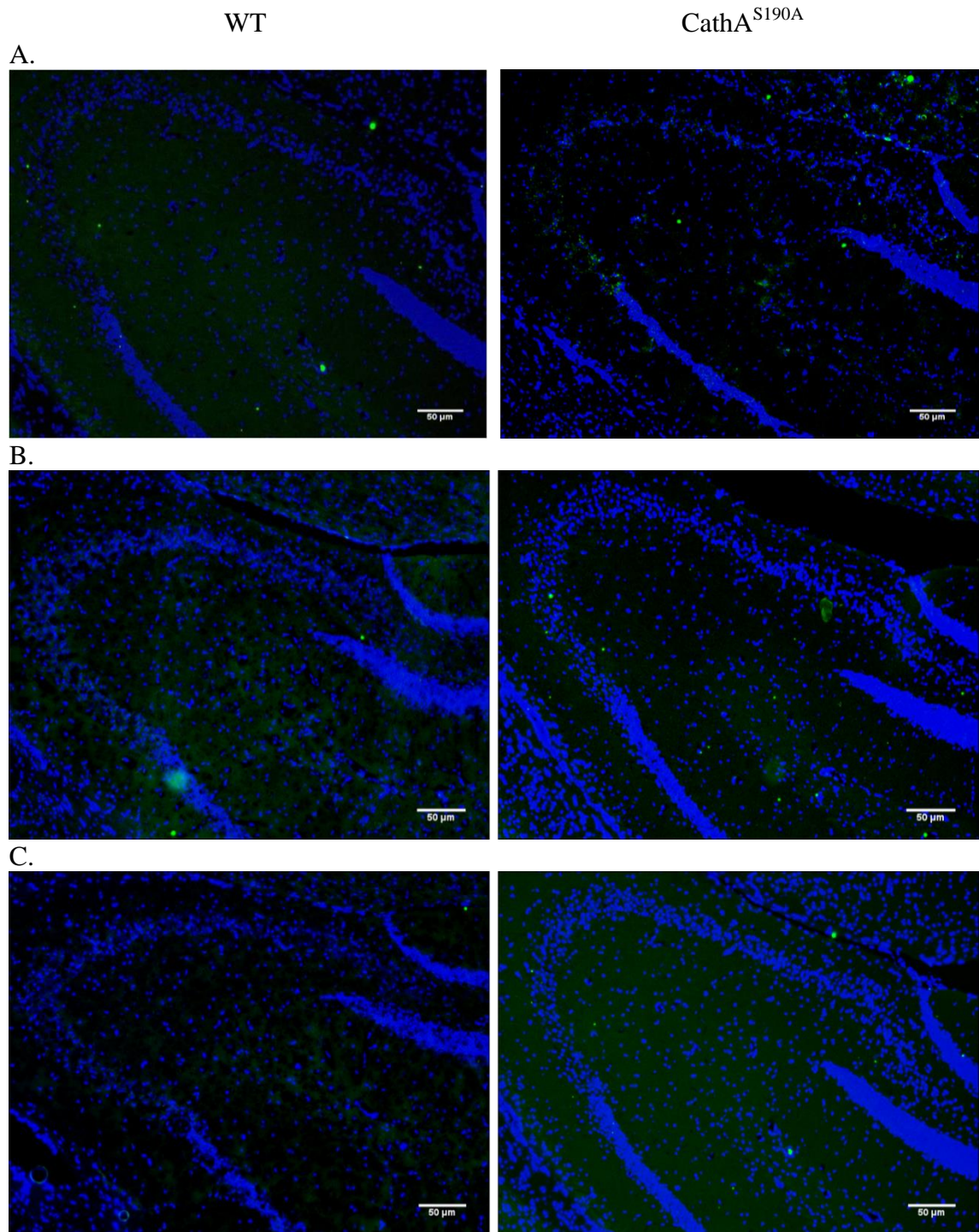
Figure 3.17 Hippocampal Substance P distribution in 3-month-old CathA^{S190A} mice and
          wild-type littermates. Images show the hippocampi of 3-month-old wild-
          type littermates and CathA^{S190A} animals after staining with Substance P
          antibody and DAPI. 3 animals are shown per genotype. A. Animal 1; B
          Animal 2; C. Animal 3. Images were taken at 20 x magnification. No cells
   were labeled when the primary antibody was omitted.
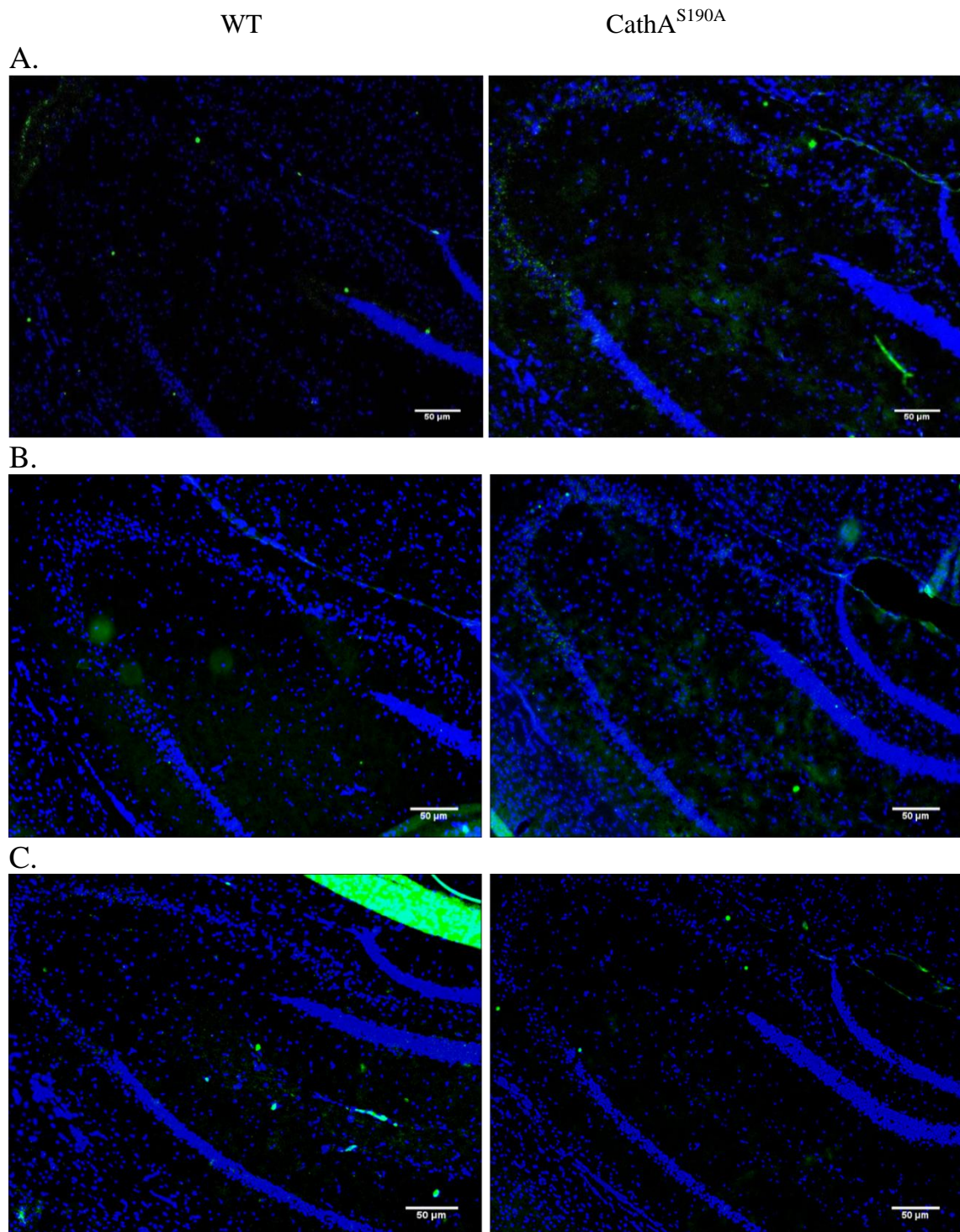
WT CathA^{S190A}

Figure 3.18 Hippocampal Substance P distribution in 6-month-old CathA^{S190A} mice and wild-type littermates. Images show the hippocampi of 6-month-old wild-type littermates and CathA^{S190A} animals after staining with Substance P antibody and DAPI. 3 animals are shown per genotype. A. Animal 1; B Animal 2; C. Animal 3. Images were taken at 20 x magnification. No cells were labeled when the primary antibody was omitted.
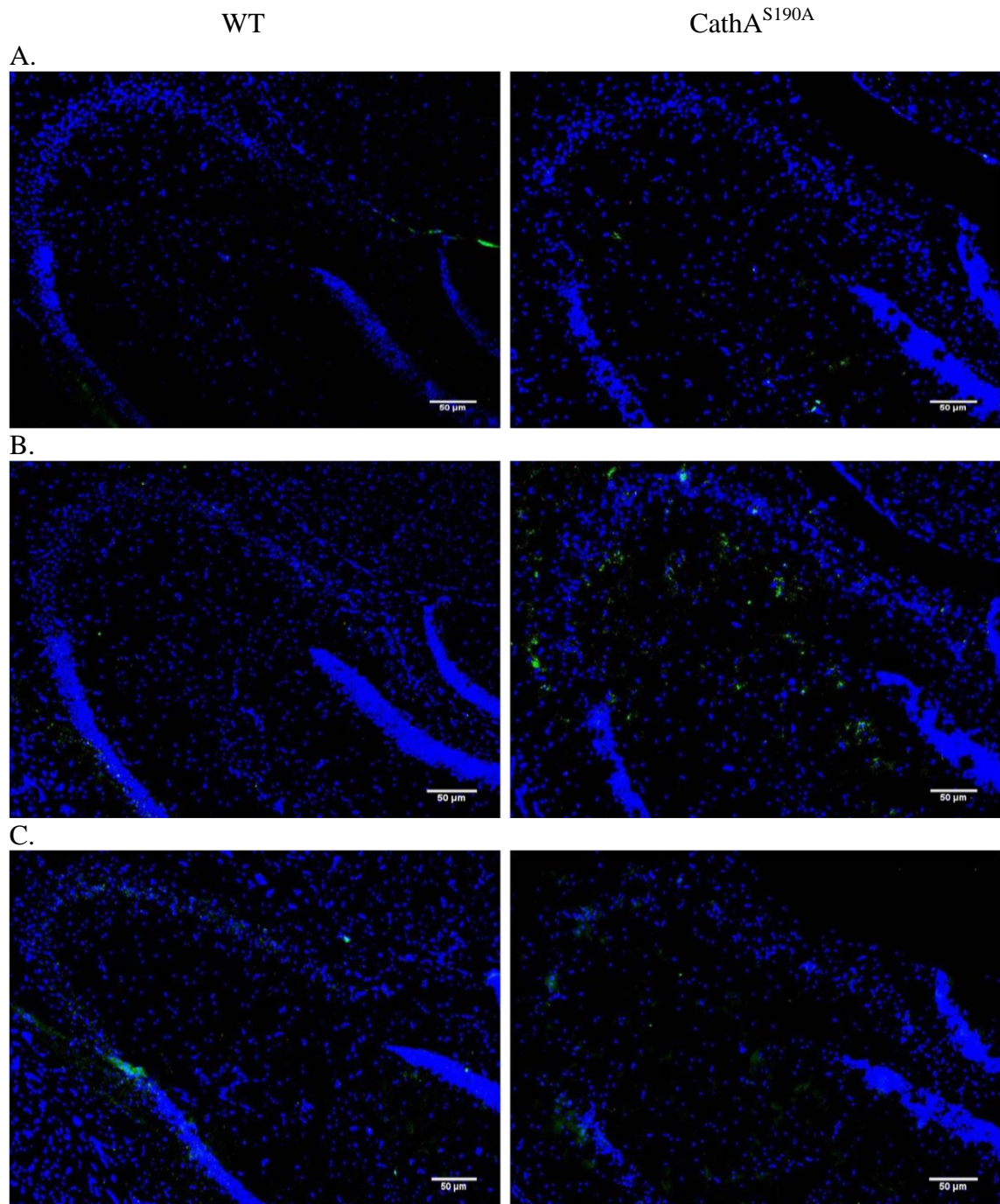
Figure 3.19 Hippocampal Substance P distribution in 12-month-old CathA^{S190A} mice and wild-type littermates. Images show the hippocampi of 12-month-old wild-type littermates and CathA^{S190A} animals after staining with Substance P antibody and DAPI. 3 animals are shown per genotype. A. Animal 1; B Animal 2; C. Animal 3. Images were taken at 20 x magnification. No cells were labeled when the primary antibody was omitted.

3.3. Behavioral Analysis

Behavioral research studies use animals as models to understand changes in the human mind and behavior, particularly for conditions involving psychiatric disorders and neurological diseases. Animals are subjected to experiments to monitor cognitive and mental illnesses, memory disorders or physiological deficiencies directly linked to aberrations in sensory and central nervous system. In this study three carefully chosen tests were applied to investigate the behavioral differences between CathA^{S190A} and wild-type littermates.

3.3.1. Evaluation of Motor Coordination in CathA^{S190A} Mice Model

To better understand the reason for the accumulation of peptides in the hippocampus, the Rotarod test was conducted (Figure 3.20). Motor function assessed by the Rotarod test showed no significant difference between CathA^{S190A} and wild-type littermates in the 3- and 6-month old groups (wild-type = 66.48 ± 4.43; CathA^{S190A} = 69.73 ± 3.48; p=0.59). In 12-month old animals, CathA^{S190A} mice showed significantly improved rotarod performance compared to their wild-type littermates (wild-type = 57.58 ± 2.49; CathA^{S190A} = 67.46 ± 6.49; p=0.013).
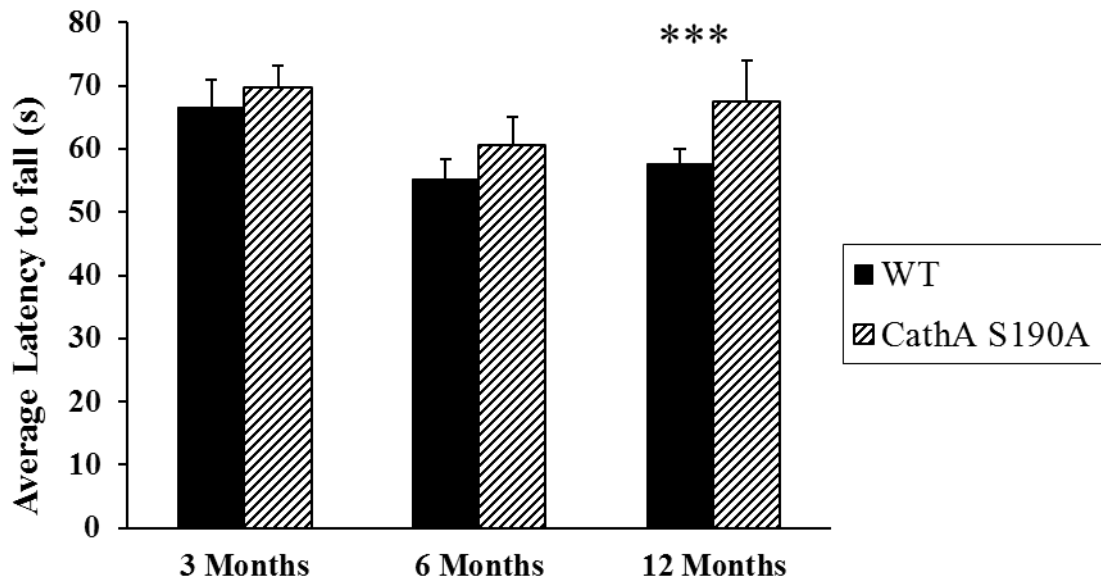
Figure 3.20 Motor activity as assessed using the rotarod paradigm. Motor activity was tested three times per day on an accelerating rotarod apparatus (4~40 rpm for 5 min). The data are presented as mean ± SEM, and significance was assessed using student t-test. 3 months old wild-type (n=11) and CathAS190A (n=18); 6 months old wild-type (n=6) and CathAS190A (n=6); 12 months old wild-type (n=9) and CathAS190A (n=15). ** = p<0.05.

3.3.2. The Influence on Cognitive Function in Passive Avoidance Step-Through Test

The effect of catalytic deficiency of CathA enzyme on memory deficit was investigated by using the passive avoidance test (Figure 3.21). There was a trend towards a shorter time for the CathA^{S190A} mice to re-enter the dark compartment on test day compared to their wild-type littermate groups (wild-type = 300 s; CathA^{S190A} = 235.46 s ± 29.11; p=0.07). The latency time of the 6-month-old CathA^{S190A} group was also approaching a borderline significant decrease in re-entry time compared with that of the wild-type group (wild-type = 300 s; CathA^{S190A} = 248.87 ± 27.34 s; p=0.11). However, at 12-months there was an almost significant difference between CathA^{S190A} and wild-type groups (wild-type = 300 s; CathA^{S190A} = 232.54 ± 35.94 s; p=0.08). Overall, the 3-months- and 6-months-old wild-type group declined to re-enter the dark

compartment under light-induced conditions, whereas the CathA^{S190A} mice group showed the same pattern of deterioration in memory function in all age groups.
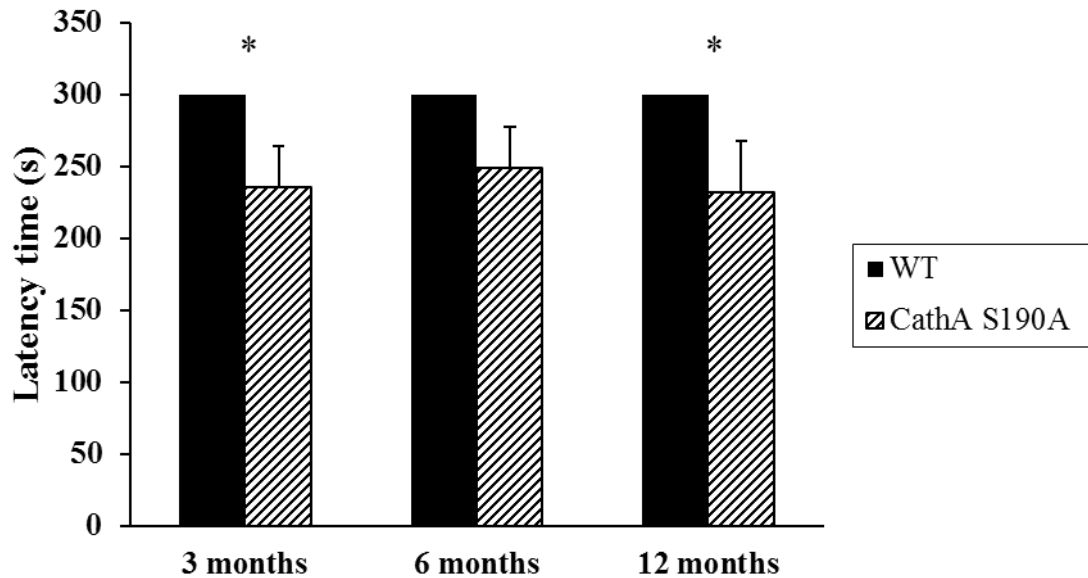
Figure 3.21 Results from the passive avoidance task assessing potential memory loss in CathA^{S190A} mice. Graphs compare latency time for mice to enter the dark compartment on the test day. If mice did not move into the dark compartment within five minutes, a latency time of five minutes was recorded. The data are presented as mean ± SEM, and significance was assessed using the student t-test. 3 months old wild-type (n=6) and CathA^{S190A} (n=6); 6 months old wild-type (n=8) and CathA^{S190A} (n=10); 12 months old wild-type (n=9) and CathA^{S190A} (n=11). * = $0.05 < p < 0.1$.

3.3.3. Effects of Enzymatic Deficiency of CathA Enzyme on Spatial Learning and Memory

Spatial learning and memory of the CathA^{S190A} mice was tested with the Morris Water Maze test in 3, 6- and 12-month old animals. Spatial memory protocols were applied in which the escape platform was placed at fixed locations into the pool relative to visual distal cues in the experiment room. The animals were placed into the pool facing towards the side of the pool from different starting positions each experimental

day. They learnt to swim to the escape platform with decreasing escape latencies and by choosing more direct paths with the help of visual distal cues hung around the sides of the room. A tracking software program supported by a video camera was used to measure parameters including path-length and swim speed (Sutherland et al. 1983). Another accepted method to measure learning ability of animals is to analyze average swim distance of animals in the pool. It is expected that mice should learn the shortest pathway to the located platform in training sessions during the 8-day experiment. However, there are some limitations to these two methods. By measuring the latency, it may give false data thief the animal chooses to wait before moving and then begins to swim towards the target directly in a short period of time. In addition, using only the moved distance may also give inaccurate data if the animal moves a short distance in the pool, yet is unable to find the platform. In order to overcome these hurdles, the measurement of proximity strategy has been used. This strategy optimizes the position of the mice with respect to the target location and provides a record of the distance from the platform, thus giving a better idea of how close the animal is to the platform during its search (Gallagher et al. 1993).

After all training procedures are completed, a probe trial is applied, in which the submerged hidden escape platform is removed from the pool and the animals are allowed to swim for 60 seconds. A well-trained animal is expected to swim immediately towards to the target quadrant of the pool and spend more time here, looking for the removed platform repeatedly before searching elsewhere. Animals with defects in the hippocampus and dentate gyrus or combined physiological deficiencies score poorly in probe trials (Morris et al. 1982).

3.3.3.1. 3-Month-Old Animals

In 3-month-old-mice, the test showed that the spatial learning and memory capability of CathA^{S190A} mice was decreased at the end of the 8-day test session. The wild-type group learnt to read the visual clues faster to reach the visible escape platform in the first 3 days, whereas CathA^{S190A} mice took a longer time to swim towards to the platform. After submerging the platform under the water from day-4, both groups had

difficulties to detect the exact location of the platform in the pool. However, both groups quickly improved their abilities to find the direction to the platform. Though wild-type mice were able to better orient themselves as the daily trials progressed, CathA^{S190A} mice showed a decreasing ability to do so (Figure 3.22). In addition to latency, the wild-type group learnt shorter paths to the platform in the first 3-days of training, whereas it can been seen that CathA^{S190A} mice swam further distances before reaching the platform (Figure 3.23). Overall CathA^{S190A} animals swam significantly longer distances in the pool in search of the platform $F (1, 269) =8, 06, p=0.005$. Proximity to the target measurements also support the fact that wild-type animals orient themselves in the pool significantly closer to the platform in their search, $F(1,251)= 16,25$ $p < 0.0001$ (Figure 3.24).

.

Figure 3.22 Learning and memory ability in 3 months old wild-type (n=7) and CathA^{S190A} (n=8) mice. Comparison of Morris water maze test results for CathA^{S190A} and wild-type littermates mice at 3 months of age. Average escape latency in the visible platform test on days 1-3, escape latency in the hidden platform test on days 4–8. 3 animals in the control group and 2 animals in the CathA^{S190A} group which refused to swim during all trials on the same day were disregarded from the experiment. Graph shows average escape time ± standard error of the mean.

Figure 3.23 Learning and memory ability in 3 months old wild-type (n=7) and CathA^{S190A} (n=8) mice. Comparison of Morris water maze test results for CathA^{S190A} and wild-type littermates mice at 3 months of age. Average moved distance in the visible platform test on days 1-3, moved distance in the hidden platform test on days 4–8. 3 animals in the control group and 2 animals in the CathA^{S190A} group which refused to swim during all trials on the same day were disregarded from the experiment. Graph shows average moved distance to target ± standard error of the mean.

Figure 3.24 Learning and memory ability in 3 months old wild-type (n=7) and CathA^{S190A} (n=8) mice. Comparison of Morris water maze test results for CathA^{S190A} and wild-type littermates mice at 3 months of age. Average search proximity of animals to the platform in the visible platform test on days 1-3, search proximity of animals in the hidden platform test on days 4–8. 3 animals in the control group and 2 animals in the CathA^{S190A} group which refused to swim during all trials on the same day were disregarded from the experiment. Graph shows average search proximity ± standard error of the mean.

3.3.3.2. 6-Month-Old Animals

In 6-months-old animals, generally the wild-type mice and CathA^{S190A} mice had a parallel learning pattern but with a different learning pace. They gave similar cognitive reactions to changes of the distal clues. CathA^{S190A} animals still demonstrated slower adaptive abilities to changing visual patterns than the control groups (Figure 3.25). The average distance needed by wild-type animals to find the platform was significantly less than their CathA^{S190A} littermates, $F_{(1,341)} = 10, 47$, $p = 0.001$ (Figure 3.26). The proximity to the platform measurement demonstrates that wild-type animals used distal clues in a better way to stay nearer to the platform than CathA^{S190A} animals, $F_{(1,382)} = 20,69$ $p < 0.0001$ (Figure 3.27).

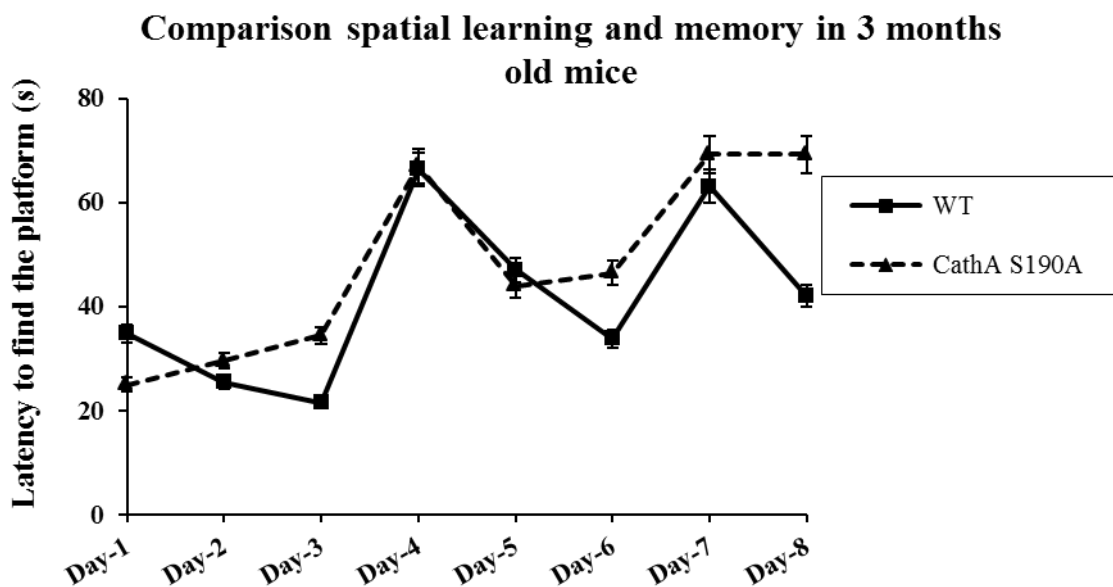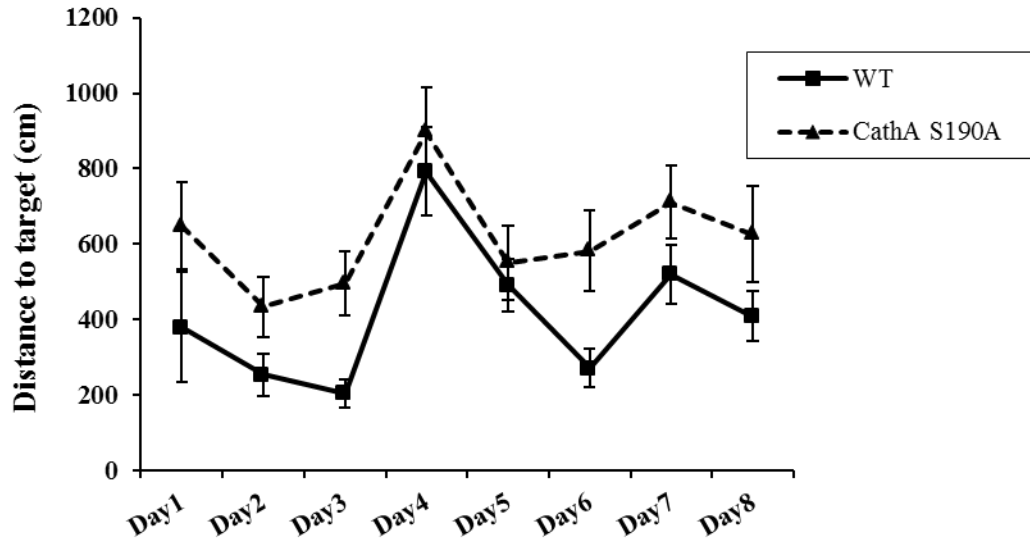**Comparison spatial learning and memory in 6 months old mice**

Figure 3.25 Learning and memory ability in 6 months old wild-type (n=8) and CathA^{S190A} (n=8) mice. Comparison of Morris water maze test results for CathA^{S190A} and wild-type littermates mice at 6 months of age. Graph shows average escape latency in the visible platform test on days 1-3, escape latency in the hidden platform test on days 4-8. 2 animals in the wild-type group and 2 animals in CathA^{S190A} group which refused to swim during all trials on the same day were disregarded from the experiment. Graph shows average distance to target ± standard error of the mean.
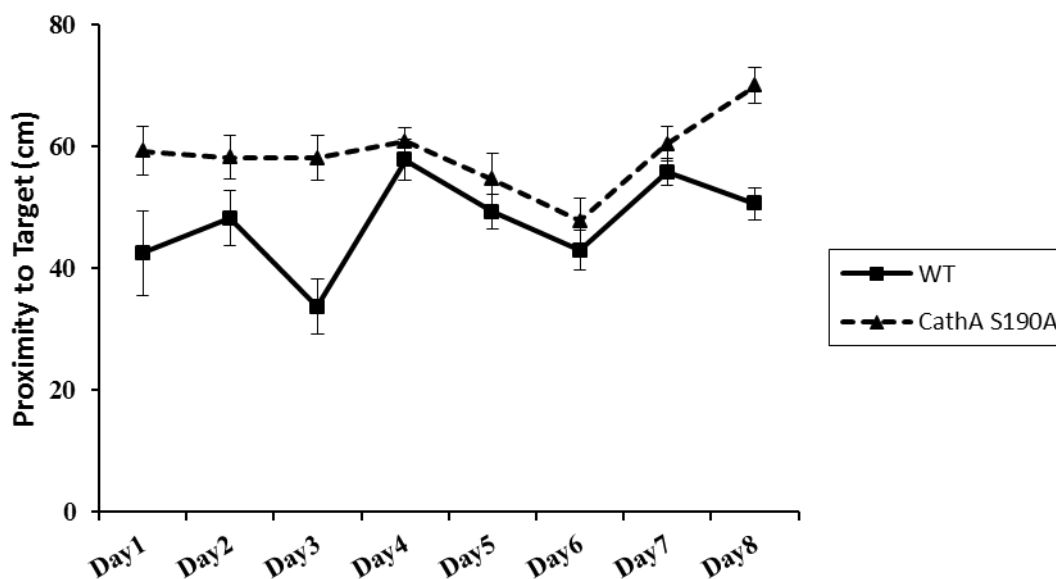
Figure 3.26 Learning and memory ability in 6 months old wild-type (n=8) and CathA^{S190A} (n=8) mice. Comparison of Morris water maze test results for CathA^{S190A} and wild-type littermates mice at 6 months of age. Graph shows average moved distance in the visible platform test on days 1-3, moved distance in the hidden platform test on days 4-8. 2 animals in the wild-type group and 2 animals in CathA^{S190A} group which refused to swim during all trials on the same day were disregarded from the experiment. Graph shows average moved distance to target ± standard error of the mean.

Figure 3.27 Learning and memory ability in 6 months old wild-type (n=8) and CathA^{S190A} (n=8) mice. Comparison of Morris water maze test results for CathA^{S190A} and wild-type littermates mice at 6 months of age. Graph shows average search proximity of animals in the visible platform test on days 1-3, search proximity of animals in the hidden platform test on days 4-8. 2 animals in the wild-type group and 2 animals in CathA^{S190A} group which refused to swim during all trials on the same day were disregarded from the experiment. Graph shows average search proximity of animals to target ± standard error of the mean.

3.3.3.3. 12-Month-Old Animals

At 12 months of age, the escape latency for both groups over the first 3 days of the experiment continuously decreased compared to previous days. Wild-type groups adapted to the submerged platform position in the pool better than CathA^{S190A} mice on day-4. After this point CathA^{S190A} mice improved scores until day-8, but never managed to reach escape latencies as fast as the wild-type groups (Figure 3.28). It can clearly be seen that 12 month wild-type animals swam less distance in the pool than their CathA^{S190A} counterparts on each day. After day-4, wild-type animals clearly showed that they followed straight paths to the platform while CathA^{S190A} littermates were swimming longer distances in the pool to reach the platform, F (1,413) = 21, 44, p < 0.0001 (Figure3.29). Even though the proximity results show that wild-type and

CathA^{S190A} animals swam nearly equal distances away from the platform, overall wild-type animals had significantly better scores from the proximity test $F_{(1,436)}=3, 98$ p= 0.04 (Figure 3.30).

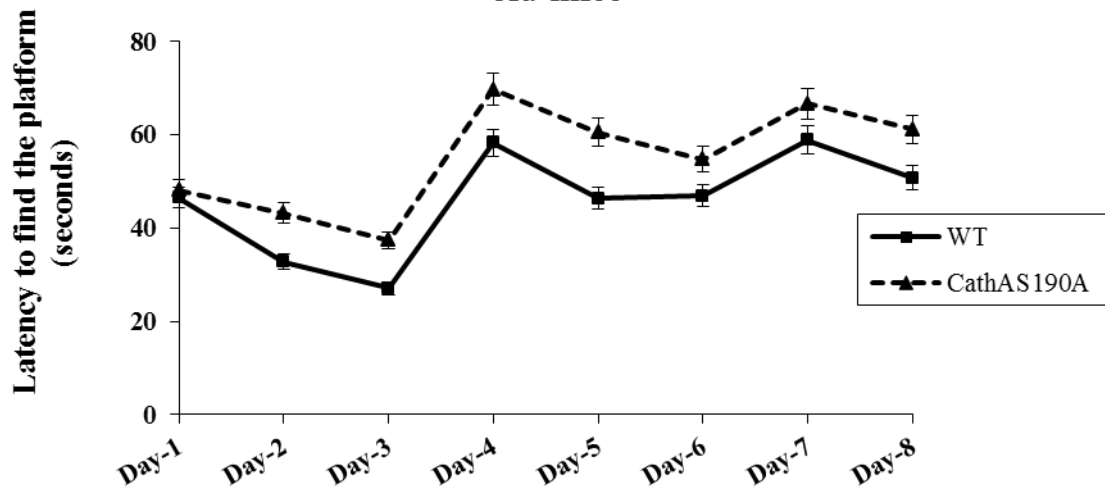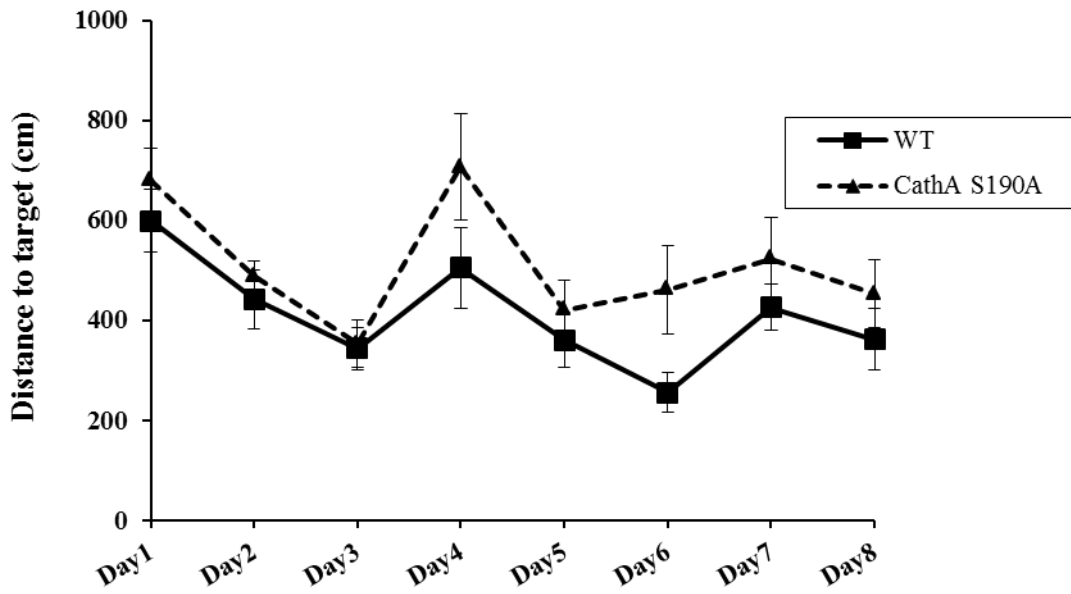**Comparison spatial learning and memory in 12 months old mice**

Figure 3.28 Learning and memory ability in 12 months old wild-type (n=7) and CathA^{S190A} (n=10) mice. Comparison of Morris water maze test results for CathA^{S190A} and control littermates mice at 12 months of age. Graph shows average escape latency (± standard error of the mean) in the visible platform test on days 1-3 and escape latency in the hidden platform test on days 4-8. Only 3 animals in the control group, which refused to swim during all trials on the same day were disregarded from the experiment.
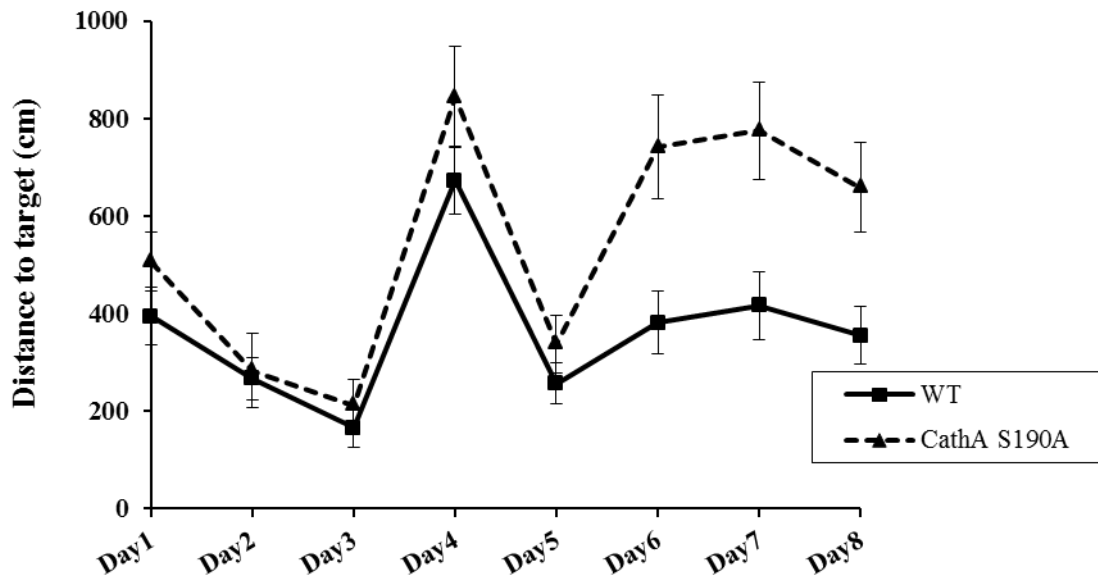
Figure 3.29 Learning and memory ability in 12 months old wild-type (n=7) and CathA^{S190A} (n=10) mice. Comparison of Morris water maze test results for CathA^{S190A} and wild-type littermates mice at 12 months of age. Graph shows average moved distance in the visible platform test on days 1-3, moved distance in the hidden platform test on days 4-8. Only 3 animals in the control group, which refused to swim during all trials on the same day were disregarded from the experiment. Graph shows average moved distance to target ± standard error of the mean.
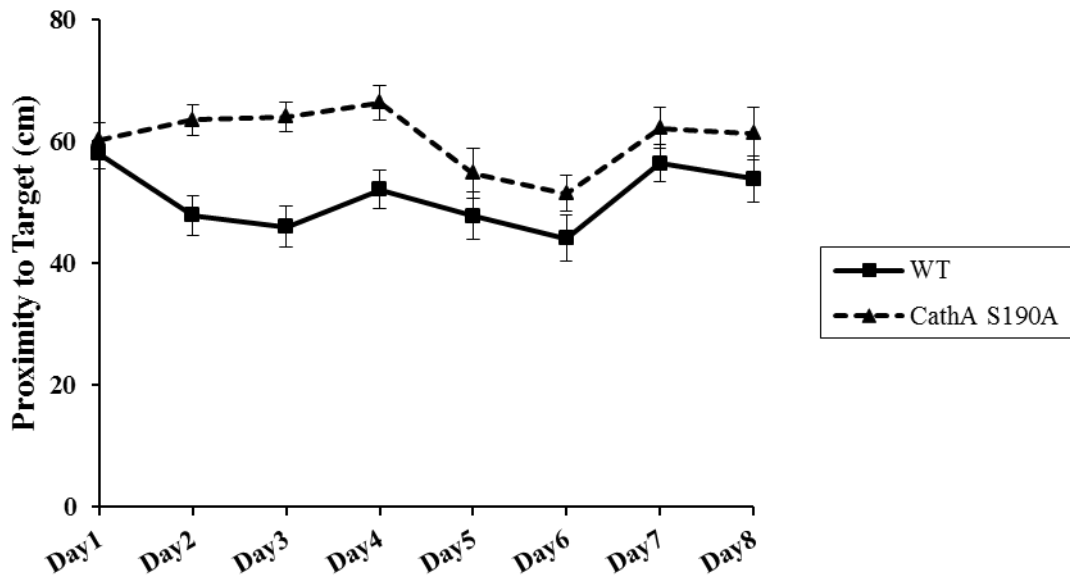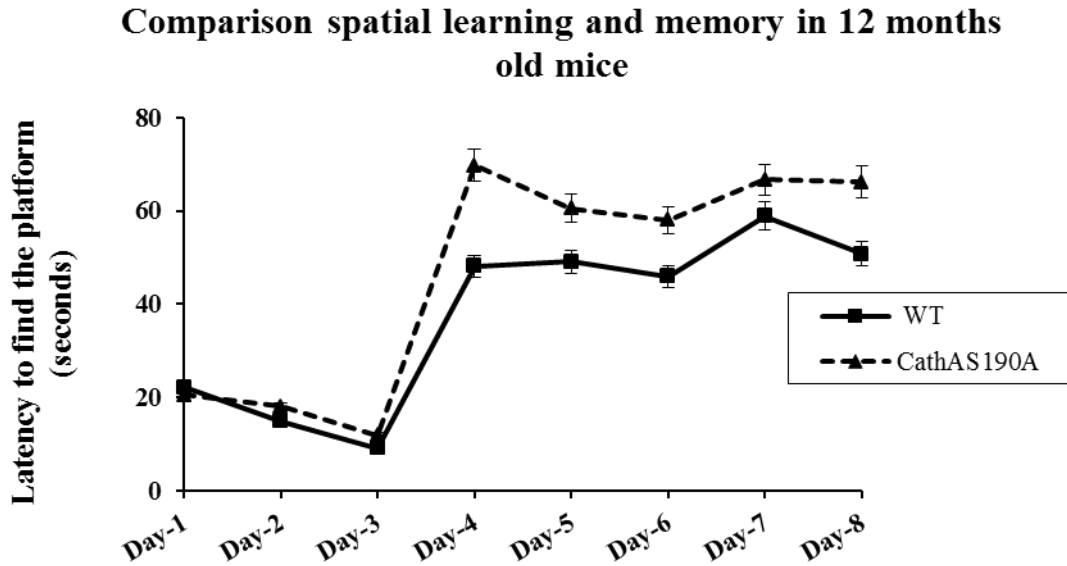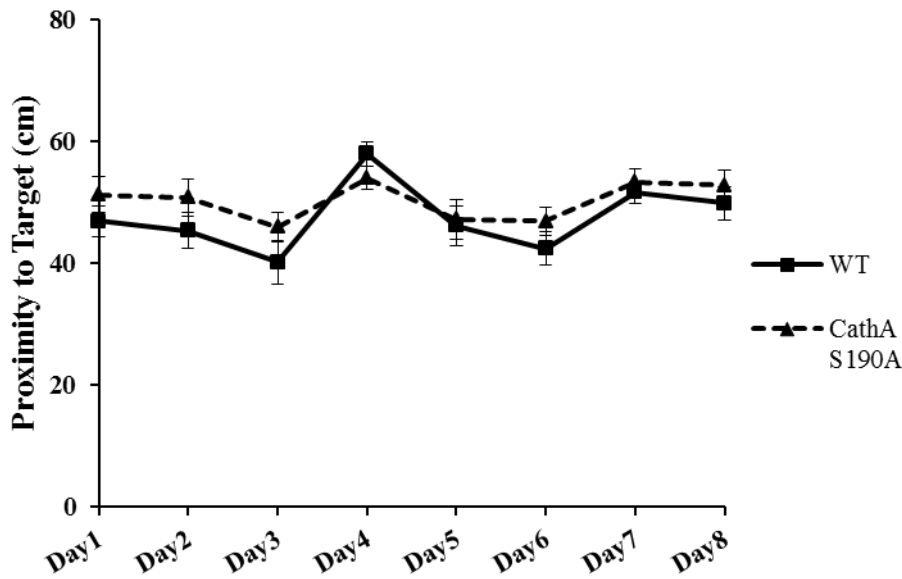
Figure 3.30 Learning and memory ability in 12 months old wild-type (n=7) and CathA^{S190A} (n=10) mice. Comparison of Morris water maze test results for CathA^{S190A} and wild-type littermates mice at 12 months of age. Graph shows average search proximity of animals in the visible platform test on days 1-3, average search proximity of animals in the hidden platform test on days 4-8. Only 3 animals in the control group, which refused to swim during all trials on the same day were disregarded from the experiment. Graph shows average search proximity of animals to target ± standard error of the mean.

To conclude, 3-month old wild-type animals spent 40 seconds, and 6, and 12-month old wild-type animals spent around 50 seconds on day 8 to find the platform after they completed their 3-day long training and 5-day long hidden platform tests. On the other hand, CathA^{S190A} littermates stayed in the pool for a significantly longer time at each age group. In the measurement of moved distance to find the platform, highly significant differences were observed between the two genotypes in all age groups. Wild-type animals continuously succeeded in finding the shortest path to the platform. In addition to these two traditional evaluation methods, we also included proximity to the platform measurement to validate our results. Proximity to the platform tests also resulted in wild-type animals performing better in all age groups. Overall, wild-type animals obtained better scores during training days, which indicates CathA^{S190A} animals struggled to learn the platform's position when compared with wild-type littermates. In addition to training days, after the platform was submerged under the water CathA^{S190A}

mice again showed poorer performance to learn to read visual clues and remember the target zone in the pool. We may conclude that CathA^{S190A} animals have significant learning deficiencies and spatial memory loss.

3.3.3.4.   Probe Trial

The probe trial was applied after animals completed both 3- day long training session and 5- day long test sessions on day 8. The aim of the trial was to understand whether animals found their ways to the previously located platform on day 8 by orienting themselves in relation to the environmental cues or in fact locating the platform was a coincidence. In this trial both traditional methods, such as measuring time spent within the platform zone or total distance moved within the platform zone, and relatively new and widely accepted method of using a measure of proximity to the goal in the analysis of probe trial was performed. The latency within the zone analysis showed that 3-, 6-, and 12- month old wild-type mice spent more time in the platform zone than CathA^{S190A} littermates (Figure 3.31). The distance taken within the zone also showed that CathA^{S190A} mice swam in the platform zone less than wild-type counterparts (Figure 3.32). In addition to these traditional methods, the measure of proximity of animals during search of platform's location indicated that wild-type animals spent their times closer to the platform position than CathA^{S190A} animals (Figure 3.33). In the light of probe trial results, we concluded that CathA^{S190A} mice have learning disability and impaired spatial memory in 3-, 6- and 12- month old animals.
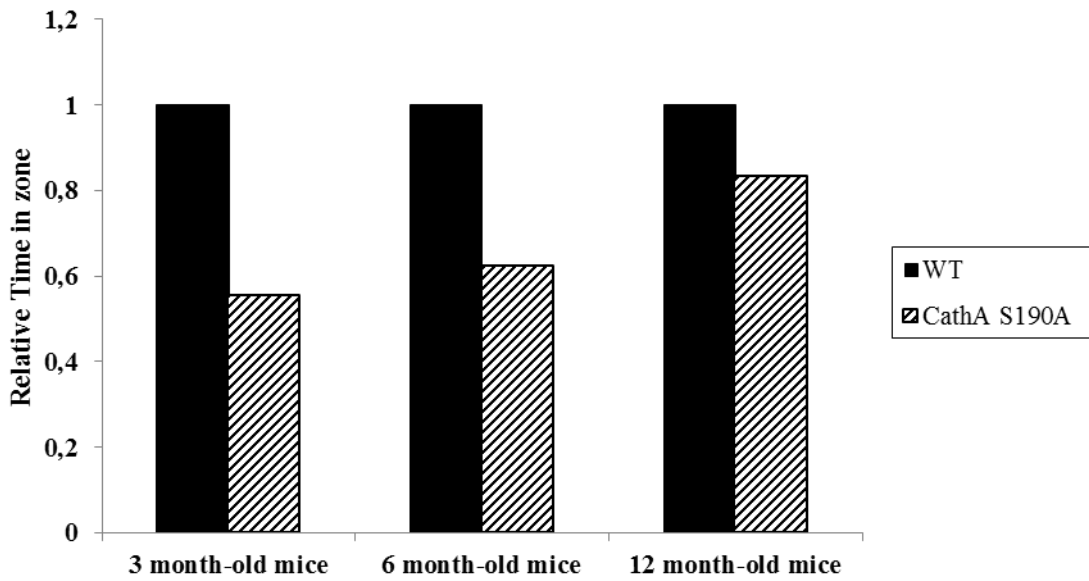
Figure 3.31 Probe trial in 3-, 6-, and 12- month old mice. Graph shows relative time spent in the platform area after the platform was removed on day 8. Only the animals which swam on all 8 days were used for the experiment. CathAS^{190A} animals were normalised to their wild-type counterparts.
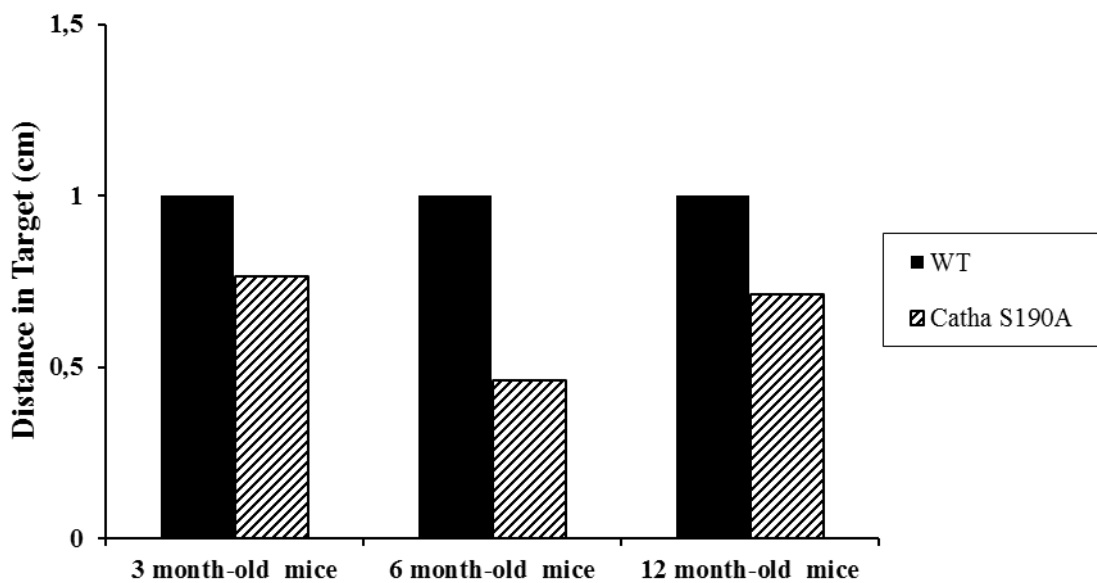
Figure 3.32 Probe trial in 3-, 6-, and 12- month old mice. Graph shows relative distance spent in the platform area after the platform was removed on day 8. Only the animals which swam on all 8 days were used for the experiment. CathAS^{190A} animals were normalised to their wild-type counterparts.
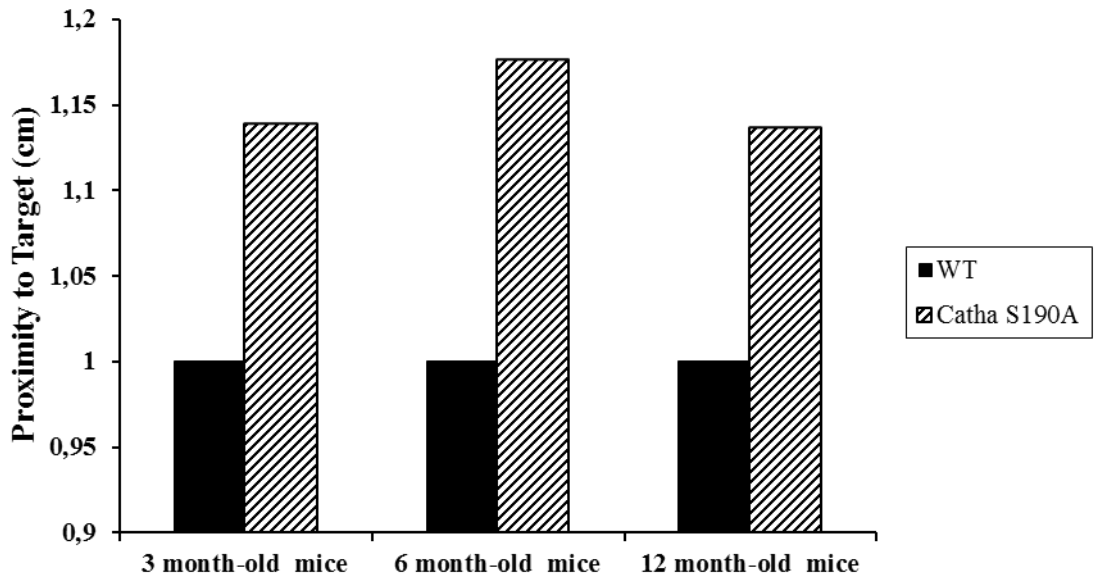
Figure 3.33 Probe trial in 3-, 6-, and 12- month old mice. Graph shows relative proximity of animals as they searched for the platform area after the platform was removed on day 8. Only the animals which swam on all 8 days were used for the experiment. CathAS[190A] animals were normalised to their wild-type counterparts.

CHAPTER 4

DISCUSSION

Lysosomal Protective Protein/ Cathepsin A (PPCA/CathA)(CathA) is a multifunctional glycoprotein that plays a role in the protection and activity of Neuraminidase-1 and β-Galactosidase, through the formation of a lysosomal multicatalytic enzyme complex (D'Azzo et al. 1982). Jackman et al used isolated CathA from platelets and lymphocytes and found that CathA possesses serine carboxypeptidase activity at acidic pH and esterase/deamidase activity at neutral pH against the carboxyl termini of a small group of vasoactive peptides, including endothelin-1, oxytocin and substance P (Jackman et al. 1990).

Catalytic activity of CathA *in vivo* was never tested at the physiological level until the generation of a catalytically inactive CathA mouse model. Previoulsy, it was demonstrated that CathA acts as an endothelin-1 inactivating enzyme (Seyrantepe et al. 2008). In this study, the regulatory function of CathA in vasoactive peptides biology has been investigated. In addition, the localization and accumulation of non-degraded forms of these peptides, including endothelin-1, oxytocin and substance P in the mice brain were studied in parallel with behavioral and cognitive outcomes.

The protective function of CathA is independent from its catalytic activity. Based on cell cultures studies, CathA was ascertained to protect both NEU1 and β-GAL from intra-lysosomal degradation by developing LMC (Caciotti et al. 2013; Hiraiwa 1999; Jackman et al. 1990). It has been demonstrated that CathA is involved in the inactivation of the lysosome-associated membrane protein type 2a (lamp2a) in chaperone-mediated autophagy (Cuervo et al. 2003).

In vitro analysis revealed the hydrolytic activity of CathA against various short peptides (Hiraiwa 1999). However, determining the *in vitro* activity of the enzyme against peptides is not enough to understand *in vivo* conditions since other molecular interactions may be involved in the regulation. A knock-out mice models of CathA was generated to evaluate the biological role of CathA. Although this animal model is well suited for mimicking symptoms of GS patients, they have severe disease symptoms

dependent on secondary enzyme deficiencies of NEU1 or β- GAL, so are not appropriate for behavioral studies such as long term memory, motor function and learning abilities. In our experiments, the gene targeted mouse, CathA^{S190A}, was used. The active CathA was replaced with a mutant enzyme carrying a Ser190Ala mutation in the enzyme active site. This mouse model expresses a catalytically inactive form of CathA protein, capable of forming lysosomal multienzyme complexes, and develops no secondary deficiencies of NEU1 or β- GAL enzymes (Seyrantepe et al. 2008).

Immunoblot analysis showed that the tissue distribution of human mature CathA differs in various different cell types and tissues, including kidney, liver, lung and brain (Table 4.1). Furthermore, immunohistochemical analysis showed that in the central nervous system CathA has strong peptidase activity (Sohma et al. 1999). Therefore, in this study we focused on the central nervous system, in particular the brain, to understand whether vasoactive peptides levels are significantly affected as a consequence of an   inactive CathA enzyme.

Table 4.1 Immunohistochemical tissue distribution of CathA. Intensity of immunohistochemical staining: + +, strong; +, moderate (adapted: Sohma et al. 1999).

Tissue	CathA Expression
Central nervous system	+ +
Liver (Hepatocytes)	+
Lung (Bronchial epithelial cells)	+ +
Kidney (Distal tubular cells, Collecting tubular cells)	+ +
Testis (Leydig's cells)	+ +

Immunofluorescence results showed that CathA deficiency results in the increased levels of endothelin-1 (Figures 3.2-3.8) and oxytocin (Figures 3.9-3.15) in the hippocampus of 3-, 6 and 12- month old mice brains. The accumulation of endothelin-1 in the hippocampal region is consistent with a demonstrated increase in the immunoreactivity in neurons and glial cells within autopsied brain regions of affected galactosialidosis human patients (Itoh et al. 2000). This data validated avidin-biotin complex immunohistochemistry methods in 3, 6 and 12 month old animal brain tissues (Figures 3.2, 3.9, 3.16).

In the future studies, using immunocytochemistry or immunocytofluorescence methods can be suitable to detect the exact cell types to understand where the peptides are exactly accumulated.

Immunofluorescence is highly specific and, one of the most well-suited and broadly accepted methods for the detection of peptides in various studies. However, an anti-Substance P antibody might be insufficient for the detection of not abundant Substance P peptide. For further analysis, mass spectrometry, which is used for more sensitive and quantitative detection of peptides, can be useful in the determination of levels of Substance P and other candidate peptides (Gillette & Carr 2013).

Furthermore, a sandwich ELISA method should be applied to confirm whether the CathA^{S190A} enzyme specificity, which has 10–15% of the carboxypeptidase activity of the wild-type enzyme, against bioactive peptides such as endothelin-1, oxytocin and substance P (Seyrantepe et al. 2008). As these peptides occur in two different forms with different amino acid sequences (i.e. a bioactive form before CathA cleavage occurs and an inactive form following CathA peptidase activity), by designing a capture antibody which is directed against the first eight amino acids (immunization and positive selection) and a detection antibody against the region around the cleavage site (negative selection), the inactive form of these short peptides can become more distinguishable.

A recent study demonstrated direct evidence that retinoid-inducible lysosomal serine carboxypeptidase 1 (Scpep1), a CathA homolog, has a complementary role to CathA in the regulation of small hormones peptides, involving endothelin-1 hydrolysis. A generated mice model with a double deficiency of both CathA and Scpep1 showed that these mice had a further reduced endothelin-1 degradation rate in the blood than

their wild-type littermates and mice singly deficient in these two enzymes. Results proved that Scpep1 and CathA are together involved in the control of endothelin-1 regulation (Pan et al. 2014). The expression of Scpep1 provides a metabolic bypass to correct endothelin-1 degradation. Similar bypass mechanisms could exist to regulate Substance P neuropeptide metabolism in the mice brain to compensate for a deficiency of CathA.

CathA deficiency also resulted in long-term deficit of learning ability in the mice model. In this study, passive avoidance tests showed that 3- and 6- month old CathA^{S190A} animals are more willing than their wild-type littermates to enter the dark chamber of the shuttle box test, despite previous foot shocks (Figure 3.21). This could be due either to an inability to create fear-associated memories, which is long term memory, or due to a lower level of fear. If it is the latter, is possible that this is a result of high level oxytocin in the hippocampus which might have longer half-life, as it avoids degradation by the inactive CathA enzyme. Previous studies have shown that exogenous application of oxytocin in both humans and rats leads to more courageous behavior and these results may have occurred through a similar mechanism (Kirsch 2005; Lee et al. 2015).

In addition, Morris Water Maze results indicated that there is clear spatial memory loss in 3-, 6- and 12- month old CathA^{S190A} animals (Figures 3.22-3.33). Orientating through the environment is a key survival skill for all organisms. The ability to learn and remember locations is associated with the use of cues outside of the organism (distal cues), allocentric navigation and the use of internal cues (proximal cues) and egocentric navigation. The hippocampus and entorhinal cortex in the mammals limbic system are the primary regions to mediate allocentric navigation. The hippocampus has been known as a significant part of the brain governing cognitive and memory functions. Lesions, long-term potentiation (LTP) problems, such as increased level of vasoactive peptides, and loss-of-function genetic mutations on signaling molecules/receptors within the hippocampus lead to impairments in spatial learning and memory. The increase in escape latency seen in the CathA^{S190A} animals, and their failure to spend more time in the correct quadrant during the probe trial, suggest that a deficiency in CathA activity leads to an impairment in spatial learning and memory.

The accumulation of endothelin-1 and oxytocin in the hippocampus of these animals may be the cause of this impairment.

These data support previously conducted experiments testing memory deficiency in a rat model in which endogenous serum CathA was immunized with human CathA. They showed that deficiency of CathA resulted in lower scores in active avoidance tests and less exploratory activities in open field tests in rat models (Ashmarin et al. 1997).

To rule out a motor impairment in these mice affecting performances in memory tasks, the motor activity of CathA^{S190A} mice was assessed using rotarod experiments (Figure 3.20). However, no significant differences were observed compared with age matched wild-type littermates.

Complex behavioral functions and cognitive abilities clearly require the function of many peptides. CathA is responsible for the regulation of many vasoactive peptides, including endothelin-1, angiotensin, bradykinin, oxytocin, substance P, neurokinin, vasopressin and corticotrophin (Hiraiwa 1999).

This investigation provides *in vivo* evidence for a regulatory role of CathA in the processing of the vasoactive peptides, endothelin-1, oxytocin and substance P in the brain. The consistent increases in the level of both endothelin-1 and oxytocin in the hippocampus of mice with an inactive CathA enzyme may suggest that there is potential redundancy in the pathways involved in vasoactive peptide metabolism in this region. The behavioral outcomes seen in these mice indicate the importance of CathA enzyme, but we cannot yet clarify whether it is directly related to the higher level of vasoactive peptide or is a more indirect consequence.

CHAPTER 5

CONCLUSION

This thesis described the physiological role of lysosomal enzyme CathA on the function of three vasoactive peptides: endothelin-1, oxytocin and substance P. In addition, changes in motor cortex activity, learning and spatial memory activity in CathA^{S190A} mice have been investigated to assess the impact of an absence of CathA hydrolytic enzyme activity.

Our immunohistochemistry results, which showed endothelin-1 accumulation in CathA^{S190A} mouse hippocampus, correlate with the previously reported distribution of this peptide in the brain tissues of galactosialidosis patients (Itoh et al. 2000) and western blot analysis results derived from the same animal model (Seyrantepe et al. 2008; Pan et al. 2014). We confirmed that endothelin-1 is a substrate for CathA, and for the first time, we showed region-specific accumulation of the peptide in mouse hippocampus in 3- month, 6- month and 12- month old groups. In addition, we showed that oxytocin is also another substrate for CathA, deficiency of which also causes accumulation of oxytocin in the hippocampus. We further investigated the accumulation pattern of Substance P in the hippocampus, however no difference was seen between CathA^{S190A} mice and their wild type litter mates in three different age groups.

Endothelin-1 and oxytocin have a broad range of roles in the regulation of cellular pathways promoting long term potentiation and long lasting spatial memory in the hippocampus (Kuwaki et al. 1997; Tomizawa et al. 2003). Therefore, in the second part of our project we investigated if abnormal accumulation of these peptides, as a result of ablating CathA hydrolytic enzyme activity, would cause any learning and memory deficits in the CathA^{S190A} mouse model. Our data showed that there is significant long term memory loss in 3- and 6- month old mice and spatial memory loss in all ages of CathA^{S190A} animals when compared with their wild-type litter mates.

The present study suggests an intriguing possibility for oxytocin, endothelin-1 and their therapeutic analogs, as novel therapeutic targets for memory loss, such as that

seen in Alzheimer's disease. If the role of these peptides in memory improvement is confirmed, development of new medical approaches to introduce oxytocin and endothelin-1 into the CNS would be beneficial in the treatment of memory-loss related diseases. In addition, as discovery of new substrates of CathA could be used as possible biomarkers in the treatment of cardiovascular diseases, such as hypertension, results from these studies will allow better understanding of lysosomal enzyme based therapeutic approaches.

BIBLIOGRAPHY

Amith, S.R. et al., 2010. Neu1 desialylation of sialyl α-2,3-linked β-galactosyl residues of TOLL-like receptor 4 is essential for receptor activation and cellular signaling. *Cellular Signalling*, 22(2), pp.314–324. Available at: http://www.sciencedirect.com/science/article/pii/S0898656809002885.

Arabkhari, M. et al., 2010. Desialylation of insulin receptors and IGF-1 receptors by neuraminidase-1 controls the net proliferative response of L6 myoblasts to insulin. *Glycobiology*, 20 (5), pp.603–616. Available at: http://glycob.oxfordjournals.org/content/20/5/603.abstract.

Ashmarin, I.P. et al., 1997. Learning disability in rats induced by the immunosuppression of cathepsin A in blood plasma. *Neuroscience Research Communications*, 21(2), pp.153–162.

Blokland, A., Geraerts, E. & Been, M., 2004. A detailed analysis of rats' spatial memory in a probe trial of a Morris task. *Behavioural Brain Research*, 154(1), pp.71–75.

Bonten, E. et al., 1996. Characterization of human lysosomal neuraminidase defines the molecular basis of the metabolic storage disorder sialidosis. *Genes and Development*, 10, pp.3156–3169.

Bonten, E.J. et al., 2009. Heterodimerization of the Sialidase NEU1 with the Chaperone Protective Protein/Cathepsin A Prevents Its Premature Oligomerization. *Journal of Biological Chemistry*, 284 (41), pp.28430–28441. Available at: http://www.jbc.org/content/284/41/28430.abstract.

Bonten, E.J., Annunziata, I. & D'Azzo, A., 2014. Lysosomal multienzyme complex: Pros and cons of working together. *Cellular and Molecular Life Sciences*, 71(11), pp.2017–2032.

Bonten, E.J. & d'Azzo, A., 2000. Lysosomal Neuraminidase: Catalytic Activation In Insect Cells Is Controlled By The Protective Protein/Cathepsin A . *Journal of Biological Chemistry*, 275 (48), pp.37657–37663. Available at: http://www.jbc.org/content/275/48/37657.abstract.

Breton, C. & Zingg, H.H., 1997. Expression and Region-Specific Regulation of the Oxytocin Receptor Gene in Rat Brain. *Endocrinology*, 138(5), pp.1857–1862. Available at: http://dx.doi.org/10.1210/endo.138.5.5127.

Caciotti, A. et al., 2013. Galactosialidosis: review and analysis of CTSA gene mutations. *Orphanet journal of rare diseases*, 8(1), p.114. Available at: http://www.ojrd.com/content/8/1/114.

Caciotti, A. et al., 2011. GM1 gangliosidosis and Morquio B disease: an update on genetic alterations and clinical findings. *Biochimica et biophysica acta*, 1812(7), pp.782–790. Available at: http://www.ncbi.nlm.nih.gov/pmc/articles/PMC3210552/.

Cooper, G.M. & Hausman, R.E., 2000. *The Cell: A Molecular Approach 2nd Edition*,

Cuervo, A.M. et al., 2003. Cathepsin A regulates chaperone-mediated autophagy through cleavage of the lysosomal receptor. *The EMBO Journal*, 22(1), pp.47–59. Available at: http://emboj.embopress.org/content/22/1/47.abstract.

D'Azzo, A. et al., 2001. *GM1 gangliosidosis and Morquio B disease: an update on genetic alterations and clinical findings.*,

D'Azzo, A. et al., 1982. Molecular defect in combined beta-galactosidase and neuraminidase deficiency in man. *Proceedings of the National Academy of Sciences of the United States of America*, 79(15), pp.4535–4539. Available at: http://www.ncbi.nlm.nih.gov/pmc/articles/PMC346709/.

Davenport, A.P. et al., 2016. Endothelin. *Pharmacological Reviews* , 68 (2), pp.357–418. Available at: http://pharmrev.aspetjournals.org/content/68/2/357.abstract.

Galjart, N.J. et al., 1988. Expression of cDNA encoding the human "protective protein≓ associated with lysosomal β-galactosidase and neuraminidase: Homology to yeast proteases. *Cell*, 54(6), pp.755–764. Available at: http://www.sciencedirect.com/science/article/pii/S0092867488909993.

Galjart, N.J. et al., 1991. Human lysosomal protective protein has cathepsin A-like activity distinct from its protective function. *Journal of Biological Chemistry*, 266(22), pp.14754–14762.

Gallagher, M., Burwell, R. & Burchinal, M.R., 1993. Severity of spatial learning impairment in aging: Development of a learning index for performance in the Morris water maze. *Behavioral Neuroscience*, 107(4), pp.618–626. Available at: http://doi.apa.org/getdoi.cfm?doi=10.1037/0735-7044.107.4.618.

de Geest, N. et al., 2002. Systemic and neurologic abnormalities distinguish the lysosomal disorders sialidosis and galactosialidosis in mice. *Human Molecular Genetics* , 11 (12), pp.1455–1464. Available at: http://hmg.oxfordjournals.org/content/11/12/1455.abstract.

Gillette, M.A. & Carr, S.A., 2013. Quantitative analysis of peptides and proteins in biomedicine by targeted mass spectrometry. *Nature methods*, 10(1), pp.28–34. Available at: http://www.ncbi.nlm.nih.gov/pmc/articles/PMC3943160/.

Hinek, A. et al., 2008. Neuraminidase-1, a Subunit of the Cell Surface Elastin Receptor, Desialylates and Functionally Inactivates Adjacent Receptors Interacting with the Mitogenic Growth Factors PDGF-BB and IGF-2. *The American Journal of Pathology*, 173(4), pp.1042–1056. Available at: http://www.ncbi.nlm.nih.gov/pmc/articles/PMC2543072/.

Hiraiwa, M., 1999. Cathepsin A/protective protein: an unusual lysosomal multifunctional protein. *Cellular and molecular life sciences : CMLS*, 56, pp.894–907. Available at: http://www.ncbi.nlm.nih.gov/pubmed/11212324.

Insel, T.R., 1992. Oxytocin — A neuropeptide for affiliation: Evidence from behavioral, receptor autoradiographic, and comparative studies. *Psychoneuroendocrinology*, 17(1), pp.3–35. Available at: http://www.sciencedirect.com/science/article/pii/030645309290073G.

Itoh, K. et al., 2000. Endothelin-1 in the brain of patients with galactosialidosis: Its abnormal increase and distribution pattern. *Annals of Neurology*, 47(1), pp.122–

126. Available at: http://doi.wiley.com/10.1002/1531-8249(200001)47:1<122::AID-ANA21>3.0.CO;2-9.

Jackman, H.L. et al., 1990. A peptidase in human platelets that deamidates tachykinins. Probable identity with the lysosomal "protective protein". *Journal of Biological Chemistry* , 265 (19), pp.11265–11272. Available at: http://www.jbc.org/content/265/19/11265.abstract.

Jones, B.J. & Roberts, D.J., 1968. The quantiative measurement of motor inco-ordination in naive mice using an acelerating rotarod. *The Journal of pharmacy and pharmacology*, 20(4), pp.302–304.

Kirsch, P., 2005. Oxytocin Modulates Neural Circuitry for Social Cognition and Fear in Humans. *Journal of Neuroscience*, 25(49), pp.11489–11493. Available at: http://www.jneurosci.org/cgi/doi/10.1523/JNEUROSCI.3984-05.2005.

Kuwaki, T. et al., 1997. Physiological role of brain endothelin in the central autonomic control: From neuron to knockout mouse. *Progress in Neurobiology*, 51(5), pp.545–579.

Lee, S. et al., 2015. Oxytocin Protects Hippocampal Memory and Plasticity from Uncontrollable Stress. *Nature Publishing Group*, pp.1–9. Available at: http://dx.doi.org/10.1038/srep18540.

Liang, F. et al., 2006. Monocyte Differentiation Up-regulates the Expression of the Lysosomal Sialidase, Neu1, and Triggers Its Targeting to the Plasma Membrane via Major Histocompatibility Complex Class II-positive Compartments. *Journal of Biological Chemistry* , 281 (37), pp.27526–27538. Available at: http://www.jbc.org/content/281/37/27526.abstract.

López-Otín, C. & Bond, J.S., 2008. Proteases: Multifunctional enzymes in life and disease. *Journal of Biological Chemistry*, 283(45), pp.30433–30437.

Maroun, M. & Wagner, S., 2015. Oxytocin and Memory of Emotional Stimuli: Some Dance to Remember, Some Dance to Forget. *Biological Psychiatry*, 79, pp.203–212. Available at: http://linkinghub.elsevier.com/retrieve/pii/S0006322315006101.

Miyagi, T., 2008. Aberrant expression of sialidase and cancer progression. *Proceedings of the Japan Academy. Series B, Physical and Biological Sciences*, 84(10), pp.407–418. Available at: http://www.ncbi.nlm.nih.gov/pmc/articles/PMC3720545/.

Miyagi, T. & Yamaguchi, K., 2012. Mammalian sialidases: Physiological and pathological roles in cellular functions. *Glycobiology*, 22(7), pp.880–896. Available at: http://www.glycob.oxfordjournals.org/cgi/doi/10.1093/glycob/cws057.

Monti, E. et al., 2010. Sialidases in Vertebrates: A Family Of Enzymes Tailored For Several Cell Functions*. In D. Horton, ed. Advances in Carbohydrate Chemistry and Biochemistry. Academic Press, pp. 403–479. Available at: http://www.sciencedirect.com/science/article/pii/S0065231810640073.

Morris, R.G.M. et al., 1982. Place navigation impaired in rats with hippocampal lesions. *Nature*, 297(5868), pp.681–683. Available at: http://dx.doi.org/10.1038/297681a0.

Morris, R.G.M., 1981. Spatial localization does not require the presence of local cues. *Learning and Motivation*, 12(2), pp.239–260.

Nan, X., Carubelli, I. & Stamatos, N.M., 2007. Sialidase expression in activated human T lymphocytes influences production of IFN-γ. *Journal of Leukocyte Biology* , 81 (1), pp.284–296. Available at: http://www.jleukbio.org/content/81/1/284.abstract.

Ögren, S.O. & Stiedl, O., 2013. Passive Avoidance. In *Encyclopedia of Psychopharmacology*. Berlin, Heidelberg: Springer Berlin Heidelberg, pp. 1–10. Available at: http://link.springer.com/10.1007/978-3-642-27772-6_160-2.

Pan, X. et al., 2014. Serine Carboxypeptidase SCPEP1 and Cathepsin A Play Complementary Roles in Regulation of Vasoconstriction via Inactivation of Endothelin-1. *PLoS Genetics*, 10(2).

Piel, M.J. et al., 2014. PAIN ASSESSMENT IN ANIMAL MODELS OF OSTEOARTHRITIS. *Gene*, 537(2), pp.184–188. Available at: http://www.ncbi.nlm.nih.gov/pmc/articles/PMC3950312/.

Pshezhetsky, A. V et al., 1997. Cloning, expression and chromosomal mapping of human lysosomal sialidase and characterization of mutations in sialidosis. *Nat Genet*, 15(3), pp.316–320. Available at: http://dx.doi.org/10.1038/ng0397-316.

Pshezhetsky, A. V & Hinek, A., 2011. Where catabolism meets signalling: neuraminidase 1 as a modulator of cell receptors. *Glycoconjugate Journal*, 28(7), pp.441–452. Available at: http://dx.doi.org/10.1007/s10719-011-9350-5.

Pshezhetsky, A. V & Potier, M., 1996. Association of N-Acetylgalactosamine-6-sulfate Sulfatase with the Multienzyme Lysosomal Complex of β-Galactosidase, Cathepsin A, and Neuraminidase: POSSIBLE IMPLICATION FOR INTRALYSOSOMAL CATABOLISM OF KERATAN SULFATE . *Journal of Biological Chemistry* , 271 (45), pp.28359–28365. Available at: http://www.jbc.org/content/271/45/28359.abstract.

Risher, W.C. et al., 2014. Astrocytes refine cortical connectivity at dendritic spines. *eLife*, 3, p.e04047. Available at: http://elifesciences.org/content/3/e04047.abstract.

Schindelin, J. et al., 2012. Fiji - an Open Source platform for biological image analysis. *Nature methods*, 9(7), p.10.1038/nmeth.2019. Available at: http://www.ncbi.nlm.nih.gov/pmc/articles/PMC3855844/.

Schneider Gasser, E.M. et al., 2006. Immunofluorescence in brain sections: simultaneous detection of presynaptic and postsynaptic proteins in identified neurons. *Nature protocols*, 1(4), pp.1887–97. Available at: http://dx.doi.org/10.1038/nprot.2006.265.

Schulkin, 1999. The neuroendocrine regulation of behavior. *Cambridge (UK): Cambridge Univ. Press;*, p.x, 323 pp.

Seyrantepe, V. et al., 2008. Enzymatic activity of lysosomal carboxypeptidase (cathepsin) a is required for proper elastic fiber formation and inactivation of endothelin-1. *Circulation*, 117, pp.1973–1981.

Seyrantepe, V., Lema, P., et al., 2010. Mice Doubly-deficient in lysosomal hexosaminidase a and neuraminidase 4 show epileptic crises and rapid neuronal loss. *PLoS Genetics*, 6(9).

Seyrantepe, V., Iannello, A., et al., 2010. Regulation of Phagocytosis in Macrophages by Neuraminidase 1. *Journal of Biological Chemistry* , 285 (1), pp.206–215.

Available at: http://www.jbc.org/content/285/1/206.abstract.

Shi, X.-B. et al., 2011. miR-125b promotes growth of prostate cancer xenograft tumor through targeting pro-apoptotic genes. *The Prostate*, 71(5), pp.538–549. Available at: http://www.ncbi.nlm.nih.gov/pmc/articles/PMC3017658/.

Siklos, M., BenAissa, M. & Thatcher, G.R.J., 2015. Cysteine proteases as therapeutic targets: does selectivity matter? A systematic review of calpain and cathepsin inhibitors. *Acta Pharmaceutica Sinica B*, 5(6), pp.506–519. Available at: http://www.pubmedcentral.nih.gov/articlerender.fcgi?artid=4675809&tool=pmcentrez&rendertype=abstract.

Sohma, O. et al., 1999. Expression of protective protein in human tissue. *Pediatric neurology*, 20(5), pp.210–4. Available at: http://www.ncbi.nlm.nih.gov/pubmed/10207930\nhttp://linkinghub.elsevier.com/retrieve/pii/S0887899498001519.

van der Spoel, A., Bonten, E. & d'Azzo, A., 1998. Transport of human lysosomal neuraminidase to mature lysosomes requires protective protein/cathepsin A. *The EMBO Journal*, 17(6), pp.1588–1597. Available at: http://dx.doi.org/10.1093/emboj/17.6.1588.

Stoka, V., Turk, V. & Turk, B., 2016. Lysosomal cathepsins and their regulation in aging and neurodegeneration. *Ageing Research Reviews*. Available at: http://dx.doi.org/10.1016/j.arr.2016.04.010.

Sutherland, R.J., Whishaw, I.Q. & Kolb, B., 1983. A behavioural analysis of spatial localization following electrolytic, kainate- or colchicine-induced damage to the hippocampal formation in the rat. *Behavioural Brain Research*, 7(2), pp.133–153. Available at: http://www.sciencedirect.com/science/article/pii/0166432883901882.

Tomizawa, K. et al., 2003. Oxytocin improves long-lasting spatial memory during motherhood through MAP kinase cascade. *Nature Neuroscience*, 6(4), pp.384–390. Available at: http://www.nature.com/doifinder/10.1038/nn1023.

Turk, B. & Turk, V., 2009. Lysosomes as "suicide bags" in cell death: Myth or reality? *Journal of Biological Chemistry*, 284(33), pp.21783–21787.

Turk, V., Turk, B. & Turk, D., 2001. Lysosomal cysteine proteases: Facts and opportunities. *EMBO Journal*, 20(17), pp.4629–4633.

Uemura, T. et al., 2009. Contribution of sialidase NEU1 to suppression of metastasis of human colon cancer cells through desialylation of integrin [beta]4. *Oncogene*, 28(9), pp.1218–1229. Available at: http://dx.doi.org/10.1038/onc.2008.471.

Vaccari, C., Lolait, S.J. & Ostrowski, N.L., 1998. Comparative Distribution of Vasopressin V1b and Oxytocin Receptor Messenger Ribonucleic Acids in Brain. *Endocrinology*, 139(12), pp.5015–5033. Available at: http://dx.doi.org/10.1210/endo.139.12.6382.

Vorhees, C. V & Williams, M.T., 2014. Assessing Spatial Learning and Memory in Rodents. *ILAR Journal*, 55(2), pp.310–332. Available at: http://www.ncbi.nlm.nih.gov/pmc/articles/PMC4240437/.

Xu, D. et al., 1994. ECE-1: A membrane-bound metalloprotease that catalyzes the proteolytic activation of big endothelin-1. *Cell*, 78(3), pp.473–485. Available at:

http://www.sciencedirect.com/science/article/pii/0092867494904251.

Yanagisawa, M. et al., 1988. A novel potent vasoconstrictor peptide produced by vascular endothelial cells. *Nature*, 332(6163), pp.411–415. Available at: http://dx.doi.org/10.1038/332411a0.

Yogalingam, G. et al., 2016. Neuraminidase 1 Is a Negative Regulator of Lysosomal Exocytosis. *Developmental Cell*, 15(1), pp.74–86. Available at: http://dx.doi.org/10.1016/j.devcel.2008.05.005.

Yu, Y. et al., 2014. Similar effects of substance P on learning and memory function between hippocampus and striatal marginal division. *Neural Regeneration Research*, 9(8), pp.857–863. Available at: http://www.ncbi.nlm.nih.gov/pmc/articles/PMC4146251/.

Zhou, X.Y. et al., 1995. Mouse model for the lysosomal disorder galactosialidosis and correction of the phenotype with overexpressing erythroid precursor cells. *Genes & Development* , 9 (21), pp.2623–2634. Available at: http://genesdev.cshlp.org/content/9/21/2623.abstract.